EBioMedicine 45 (2019) 588–605

Contents lists available at ScienceDirect

EBioMedicine

journal homepage: www.ebiomedicine.com

EBioMedicine
Published by THE LANCET

Research paper

Fibrates as drugs with senolytic and autophagic activity for osteoarthritis therapy

Uxía Nogueira-Recalde [a], Irene Lorenzo-Gómez [a], Francisco J. Blanco [a], María I. Loza [b], Diego Grassi [c], Valery Shirinsky [d], Ivan Shirinsky [d], Martin Lotz [e], Paul D. Robbins [f], Eduardo Domínguez [b,**], Beatriz Caramés [a,*]

[a] Uxía Nogueira-Recalde, Irene Lorenzo Gómez, Francisco J. Blanco and Beatriz Caramés, Grupo de Biología del Cartílago, Servicio de Reumatología, Instituto de Investigación Biomédica de A Coruña (INIBIC), Complejo Hospitalario Universitario de A Coruña, Sergas, A Coruña, Spain
[b] Eduardo Domínguez: Biofarma Research Group, Center for Research in Molecular Medicine and Chronic Diseases (CIMUS), Universidad de Santiago de Compostela, Spain
[c] Institute for Interdisciplinary Neuroscience (IINS), Bordeaux, Nouvelle-Aquitaine, France
[d] Scientific Research Institute of Clinical immunology, Novosibirsk, Russia
[e] Department of Molecular Medicine, Scripps Research, La Jolla, CA, USA
[f] Institute on the Biology of Aging and Metabolism, Department of Biochemistry, Molecular Biology and Biophysics, University of Minnesota, Minneapolis, MN, USA

ARTICLE INFO

Article history:
Received 16 May 2019
Received in revised form 21 June 2019
Accepted 25 June 2019
Available online 5 July 2019

Keywords:
Senescence
Autophagy
Screening
Therapeutics
Ageing
Osteoarthritis

ABSTRACT

Background: Ageing-related failure of homeostasis mechanisms contributes to articular cartilage degeneration and osteoarthritis (OA), for which disease-modifying treatments are not available. Our objective was to identify molecules to prevent OA by regulating chondrocyte senescence and autophagy.
Methods: Human chondrocytes with IL-6 induced senescence and autophagy suppression and SA-β-gal as a reporter of senescence and LC3 as reporter of autophagic flux were used to screen the Prestwick Chemical Library of approved drugs. Preclinical cellular, tissue and blood from OA and blood from OA and ageing models were used to test the efficacy and relevance of activating PPARα related to cartilage degeneration.
Findings: Senotherapeutic molecules with pro-autophagic activity were identified. Fenofibrate (FN), a PPARα agonist used for dyslipidaemias in humans, reduced the number of senescent cells *via* apoptosis, increased autophagic flux, and protected against cartilage degradation. FN reduced both senescence and inflammation and increased autophagy in both ageing human and OA chondrocytes whereas PPARα knockdown conferred the opposite effect. Moreover, PPARα expression was reduced through both ageing and OA in mice and also in blood and cartilage from knees of OA patients. Remarkably, in a retrospective study, fibrate treatment improved OA clinical conditions in human patients from the Osteoarthritis Initiative (OAI) Cohort.
Interpretation: These results demonstrate that FDA-approved fibrate drugs targeting lipid metabolism protect against cartilage degeneration seen with ageing and OA. Thus, these drugs could have immediate clinically utility for age-related cartilage degeneration and OA treatment.
Fund: This study was supported by Instituto de Salud Carlos III- Ministerio de Ciencia, Innovación y Universidades, Spain, Plan Estatal 2013–2016 and Fondo Europeo de Desarrollo Regional (FEDER), "*Una manera de hacer Europa*", PI14/01324 and PI17/02059, by Innopharma Pharmacogenomics platform applied to the validation of targets and discovery of drugs candidates to preclinical phases, Ministerio de Economía y Competitividad, by grants of the National Institutes of Health to PDR (P01 AG043376 and U19 AG056278). We thank FOREUM Foundation for Research in Rheumatology for their support.

1. Introduction

Increasing evidence about the molecular mechanisms of ageing suggests that many chronic diseases such as osteoarthritis (OA) are associated with the hallmarks of ageing, including cellular senescence and defective autophagy [1]. OA is the most prevalent joint disease, and has a major impact on global health impact in the ageing population, but neither preventive measures nor disease-modifying treatments are yet available [2].

* Correspondence to: B. Caramés, Grupo de Biología del Cartílago, Servicio de Reumatología, Instituto de Investigación Biomédica de A Coruña (INIBIC), Complejo Hospitalario Universitario de A Coruña, Sergas, As Xubias, 84 15006 A Coruña, Spain.
** Correspondence to: E. Domínguez, Biofarma Research Group, Center for Research in Molecular Medicine and Chronic Diseases (CIMUS), Universidad de Santiago de Compostela, Avenida de Barcelona s/n 15782 Santiago de Compostela, Spain.
E-mail addresses: eduardo.dominguez@usc.es (E. Domínguez), beatriz.carames.perez@sergas.es (B. Caramés).

https://doi.org/10.1016/j.ebiom.2019.06.049

Research in context

Evidence before this study

Ageing is a major risk factor in patients with cartilage degeneration and Osteoarthritis (OA). Selective targeting of senescent chondrocytes provides beneficial effects by attenuating inflammation and enhancing structural support of articular cartilage. Small molecules capable of eliminating chondrocytes with senescence features might prevent cartilage dysfunction related to ageing.

Added value of this study

In this study, we screened for compounds that both decrease senescence and increase autophagy by a cell-based high-throughput screening (HTS) in human chondrocytes. Importantly, we have identified Fenofibrate, a PPARα agonist targeting lipid metabolism, as a potential treatment against cartilage ageing and OA. OA patients treated with fibrates have improved physical functions and therefore better mobility (human cohort study).

Implications of all the available evidence

This study provides novel evidence that activating PPARα by fibrates prevent cartilage degradation by modulating key mechanisms such as senescence and autophagy in chondrocytes and cartilage. Collectively, our data establish that fibrates could be translated into disease-modifying therapeutics for OA patients.

Accumulation of senescent cells in tissues contributes to age-related diseases [3–7]. Articular cartilage of patients with OA shows features of senescence, including increased expression of nitric oxide, pro-inflammatory cytokines, particularly IL-1β [8]; p16 [9]; activated DNA damage response; ROS secretion and SA-β-Gal activity [10]. Senescence-associated secretory phenotype (SASP) factors released from chondrocytes, such as pro-inflammatory cytokines and extracellular matrix degrading enzymes, have been identified as major mediators contributing to the development and progression of OA [11,12]. Similarly, intra-articular injection of senescent cells in mice results in OA-like pathology [13]. Cartilage ageing can be modified by selective elimination of senescent chondrocytes to prevent the detrimental microenvironment changes occurring in joint dysfunction. A major step into the translation of senolytic treatments for OA was demonstrated by the beneficial effects of selective clearance of senescence chondrocytes using the Bcl-2 family inhibitor Navitoclax in animal models [14]. Physical activity intervention in rats ameliorates the deleterious effects of chondrocyte senescence and ageing [15], indicating that cartilage degeneration responds to environmental signals. The broad impact of senolytic treatment is also highlighted by the efficacy of dasatinib and quercetin combination in several models of age-related disease, which results in an extension of healthspan and lifespan in mice [6], as well as protects from idiopathic fibrosis in a first-in-human trial [16]. Comprehensive reviews have highlighted the relevance of senescence in disease and in particular for pathogenesis of OA [17–20].

There is strong evidence linking deficient autophagy, essential for cellular homeostasis, with cartilage ageing and OA [21,22]. Given its broad clinical implications and is relevance in the pathogenesis of disease, autophagy has become a major target for drug discovery and development [23,24]. Autophagy modulation by different means is a promising therapeutic approach and the discussion is currently focused on which indication will become the first clinically approved [25]. Indeed, pharmacological activation of autophagy with small molecules has shown efficacy in preclinical models of OA [20]. Activating FoxO transcription factors protect against OA-associated cartilage damage [26]. However, targeting these homeostasis mechanisms to identify and test efficacy of potential disease-modifying treatments for cartilage ageing and OA has been proven to be challenging.

Cellular senescence and autophagy are not only essential for homeostasis but are potential therapeutic targets for age-related diseases [27]. We aim to test this therapeutic hypothesis in preclinical models of OA, where senescence and autophagy play a relevant role. A novel cell-based dual imaging screening assay was developed to identify both senotherapeutics, able to either suppress markers of senescence (senomorphics) or to induce apoptosis of senescent cells (senolytics), and autophagy modulators. Senescence was induced in the T/C28a2 human chondrocyte cell line by IL-6 treatment and the percentage of cells positive for senescence-associated β-galactosidase (SA-β-Gal) activity was quantitated using the C_{12}FDG fluorescence substrate as a reporter [28]. The Prestwick chemical library of 1120 off-patent drugs, combining high chemical and pharmacological diversity with demonstrated bioavailability and safety in humans was used to screen for senescence modulators. These were subsequently tested for autophagic flux activity in stably transfected chondrocytes using a LC3 reporter [29–31]. Among the identified compounds and mechanisms, we selected fenofibrate (FN), a peroxisome proliferator-activated receptor alpha (PPARα) agonist, that is in clinical use for the treatment of lipid metabolism dysfunction for further studies [32]. Our data provides compelling evidence that activating PPARα initiates a transcriptional program that enhances chondrocyte homeostasis. Moreover, FN and other ligands were able to prevent cartilage degradation and to positively modulate key molecular mechanisms such as senescence and autophagy in chondrocytes and cartilage. We also demonstrate that PPARα expression in mice was reduced due to ageing or OA and also in blood and cartilage from knees of OA patients. Collectively, our data establish strong preclinical evidence that could lead to the development of novel disease-modifying therapies targeting lipid metabolism to prevent and treat OA.

2. Materials and methods

2.1. Chemicals and materials

Dulbecco's Modified Eagle's Medium (DMEM, Lonza, Basel, Switzerland, cat# BE-604F), Eagle's Minimum Essential Medium (EMEM, ATCC®, cat# 30–2003), Fetal Calf Serum (FCS, Gibco by Life Technologies, CA, cat# 26010–074), FBS (Sigma-Aldrich, St. Louis, MO, cat# F9665), Penicillin-Streptomycin (P/S, Sigma-Aldrich, cat# P0781), Puromycin (Sigma-Aldrich, cat# P8833), Glutamax (Thermo Fisher Scientific, CA, cat# 35050–061), Sodium pyruvate solution (Sigma-Aldrich, cat# S8636), MEM Non-essential Amino Acid Solution (Sigma-Aldrich, cat# M7145), pBABE-puro mCherry-EGFP-LC3B (Addgene, Cambridge, MA, cat# 22418, RRID:Addgene_22418), FuGene (Promega, Spain, cat# E2691), Opti-MEM® (1×) (Thermo Fisher Scientific, cat# 11058), Hank's Balanced Salt Solution (HBSS, Sigma-Aldrich, cat# H6648), ImaGene Green™ C12FDG LacZ Gene Expression kit (Life Technologies, USA, cat# D2893), Hoechst 33342 (Thermo Fisher Scientific, cat# 62249), Paraformaldehyde (PFA, Sigma-Aldrich, cat# 158127), Annexin V-FITC Apoptosis Detection kit (Inmunostep, Spain, cat# ANXVKF-100 T), Griess Reagent (Enzo Life Sciences, Ann Arbor, MI, cat# alx-400-004-L050), Luminata™ Classico Western HRP Substrate, Millipore Corporation, MA, USA, Cat# WBLUC0100), Pierce® BCA Protein Assay (Thermo Fisher Scientific, cat# 23225), RNA isolation [Trizol (Thermo Fisher Scientific, cat# 15596026), RiboPure RNA Purification kit blood (Thermo Fisher Scientific, cat# AM1928), NZY First-Strand cDNA Synthesis kit (NZYTech, Portugal, cat# MB12501), iScript cDNA Synthesis kit (Bio-Rad, CA, cat# 1708890)], ImmPRESS DAB Reagent (Vector Labs, Burlingame, CA cat# MP-7401, RRID:AB_2336529), DAB-Peroxidase substrate Kit (Vector Labs, cat# SK-4100, RRID:AB_

2336382), Prestwick Chemical Library (Prestwick Chemical, Illkirch, France), Fenofibrate (Sigma-Aldrich, MO, cat# F6020, https://www.drugbank.ca/drugs/DB01039), GW7647 (Sigma-Aldrich, St. Louis, MO, cat# G6793, https://pubchem.ncbi.nlm.nih.gov/compound/3392731), CP775146 (Sigma-Aldrich, cat# PZ0173, https://pubchem.ncbi.nlm.nih.gov/compound/10410059), Rapamycin (Calbiochem, Germany, cat# 5053210, https://www.drugbank.ca/drugs/DB00877), Navitoclax (ChemieTek, IN, USA, cat# CT-A263, https://www.drugbank.ca/drugs/DB12340), Etoposide (Sigma, cat# E1383, https://www.drugbank.ca/drugs/DB00773), Cloroquine (CQ, Sigma-Aldrich, cat# C6628), Bafilomycin (Sigma-Aldrich, cat# B1793), Interleukin-6 (IL-6, Sigma-Aldrich, cat# SRP3096), Interleukin-1β (IL-1β, Sigma-Aldrich, cat# I9401), Tumor Necrosis Factor α (TNFα, Sigma-Aldrich, cat# T6674), Actinomycin D (Sigma-Aldrich, cat# A9415), p21 (Cell Signalling Technology, Netherlands, cat# 2947, RRID:AB_823586), p16 (Abcam, UK, cat# ab51243, RRID:AB_2059963), phospho-S6 Ribosomal Protein (prpS6, Cell Signalling Technology, cat# 4858, RRID:AB_916156), LC3 (Cell Signalling Technology, cat# 3868, RRID:AB_2137707), NFκB (Cell Signalling Technology, cat# 8242, RRID:AB_10859369), PPARα (Thermo Fisher Scientific, cat# PA1-822A, RRID:AB_2165595), α-tubulin (Sigma-Aldrich, cat# T9026, RRID:AB_477593), Horseradish peroxidase (HRP)-conjugated anti-rabbit IgG (Sigma-Aldrich, cat# NA934, RRID:AB_2722659), Horseradish peroxidase (HRP)-conjugated anti-mouse IgG (Sigma-Aldrich, cat# NA931, RRID:AB_772210), Taqman probes (Hs00797944s1 MAP1LC3 FAM, cat# 4331182, Hs00231106 m1 FOXO1 FAM, cat# 4331182, Hs00355782 m1 CDKN1A FAM, cat# 4331182, Hs05332856 s1 NFκB FAM, cat# 4351372, Hs00912671 m1 CPT1A FAM, Hs01074241 m1 ACOX1 FAM, CA, cat# 4331182, Hs00947536 m1 PPARα FAM, CA, cat# 4331182, Thermo Fisher Scientific), h36B4_592F 5´CCACGCTGCTGAACATGC3´, h36B4_658R 5´TCGAACACCTGCTGGATGAC3, Integrated DNA Technologies, IDT, CA, cat# 76583076 and cat# 76583077) and h36B4_VIC VIC-AACATCTCCCCCTTCTCCTTTGGGCT-TAMRA probe (Thermo Fisher Scientific, cat# 450024), siRNA PPARα (ID: 5439, cat# AM51331; Ambion, Austin, TX, USA), Lipofectamine RNAiMAX transfection reagent (Life Technologies, NY, USA, cat# 13778030), Silencer Cy-labelled negative Ctrl N.1 siRNA (Ambion, cat# AM4621), Echo®550 Acoustic Liquid Dispensing Technology (Labcyte, San José, CA), Janus (Perkin Elmer, USA), Multidrop™Combi Reagent Dispenser (Thermo Fisher Scientific, CA), Microplate Washer (Biotek, CA), Operetta High-Content Imaging System (Perkin Elmer, USA), Harmony® Image Analysis Software (Perkin Elmer), FACScalibur cytometer (Becton Dickinson, CA, RRID:SCR_000401), software CellQuestPro (Becton Dickinson), Amersham Imager 600 (GE Healthcare, Weltham, MA), Image J software (National Institute of Health, USA, RRID:SCR_003070), Nanoquant Infinite M200 (Tecan, Switzerland), NanoDrop ND-1000 (Thermo Fisher Scientific, RRID:SCR_016517), Thermal Cycler (Thermo Fisher Scientific), LightCycler 480 Instrument II (Roche Life Science), qBASE+ qPCR analysis software (Biogazelle, Switzerland, RRID:SCR_003370), Prism 6.0 software (GraphPad Software, La Jolla, CA, USA, RRID:SCR_002798).

2.2. T/C28a2 chondrocytes

The immortalized human juvenile chondrocyte cell line T/C28a2 [33], was cultured in DMEM supplemented with 10% FCS and 100 IU/ml Penicillin / 100 μg/ml Streptomycin at 37 °C and 5% CO_2.

2.3. Chondrocyte isolation and culture

OA human cartilage was obtained from patients undergoing knee replacement (mean ± SD: 76.8 ± 4.71 years old, $n = 5$). Normal-Ageing human cartilage was harvested at the time of autopsy from the femoral condyles and the tibia plateaus of patients who had no history of joint disease (mean ± SD: 76.1 ± 14.50 years old, $n = 10$). Cartilage slices were minced and incubated with trypsin (0.5 mg/ml) (Sigma-Aldrich, St. Louis, MO, USA) for 10 min at 37 °C, and then shaken overnight at at 37 °C with collagenase IV (Sigma-Aldrich) in DMEM with 5% FCS. The digest was centrifuged and the cells were incubated in DMEM with 10% FCS at 37 °C and 5% CO_2. Only first passage cells were used in the experiments.

2.4. Cartilage explants

Cartilage explants from human normal ageing patients (mean ± SD: 73.33 ± 17.95 years old, $n = 3$) were employed to evaluate cartilage degradation in response to IL-1β.

2.5. Samples consent statement

The samples needed to carry out this study were obtained from the collection of samples for the investigation of Rheumatic Diseases of Dr. Francisco J. Blanco García, from Xerencia de Xestion Integrada de A Coruña (XXIAC) and Instituto de Investigación Biomédica de A Coruña (INIBIC). This collection was registered in the National Registry of Biobanks, with registration code: C.0000424 and approved by the Ethics Committee of Galicia with registration code: 2013/107. The information and informed consent sheet was given to all participants in the research, whose biological samples and clinical data may be susceptible to be used in this study and are authorized by the Ethics Committee of Galicia, Law 14/2007, of the July 3, and Biomedical Research 1716/2011 of November 18. All the information obtained from the analysis of the samples will be treated at all times under the criteria of confidentiality and in accordance with the security requirements required by the Spanish legislation on data protection.

In addition, all methods were performed in accordance with the relevant guidelines and regulations and The Ethics Committee of Galicia, Spain approved this study.

2.6. Blood from the Spanish OA Cohort PROCOAC (PROspective Cohort of Osteoarthritis of A Coruña)

Total RNA was extracted from blood from Non-OA patients (Age: mean ± SD: 60.95 ± 6.51 years old, Body Mass Index (BMI): mean ± SD: 24.96 ± 3.34, Grade KL 0, Females, $n = 25$) and knee OA patients (mean ± SD: 67.42 ± 6.45 years old, BMI: mean ± SD: 29.30 ± 2.83, Grade KL 3 and 4, Females, $n = 30$) from the Spanish Cohort PROCOAC [34].

2.7. Prestwick chemical library

Prestwick chemical library was purchased from Prestwick Chemical. This collection contains 1120 pharmacological active compounds, 100% approved drugs (FDA, EMA and other agencies) selected by a team of medicinal chemists and pharmacists for their high chemical and pharmacological diversity as well as for their known bioavailability and safety in humans. The compounds were pre-dissolved at 10 mM concentration in DMSO.

2.8. Senescence-associated β-galactosidase activity screening

A Multidrop Combi Reagent Dispenser was used for seeding cells into 384-well plates (3000 cells/well; Cell Carrier, Perkin Elmer) in DMEM supplemented with 10% FCS and 1% P/S and cells were cultured until confluence. Then cells were treated in DMEM 2% FCS with IL-6 20 ng/ml or with Prestwick chemical library at 10 μM. Echo®550 Acoustic Liquid Dispensing Technology was used to add 75 nl of each sample to the interval plate. An automated workstation JANUS and liquid handling was employed to transfer 50 μl per well of IL-6 with the compounds from the interval plate to the assay plate. The final assay volume was 50 μl. To measure senescence-associated-β-galactosidase (SA-β-Gal) activity in live cells, we employed ImaGene Green™ C_{12}FDG lacZ Gene Expression Kit (C_{12}FDG) according to the supplier's

instructions. Cells were incubated with C_{12}FDG substrate reagent (30 μM) and Hoechst 33342 (2.5 μl/ml) for 1 h at 37 °C and 5% CO_2. SA-β-Gal activity was stopped with phenylethyl β-d-thiogalactoside (PETG, 1 mM) for 5 min at room temperature (RT) and cells were fixed with PFA 4% for 10 min at RT. CQ (200 μM) was employed as a negative control for SA-β-Gal activity. For data acquisition, images were captured by using the Operetta® High Content Screening system. This system is an automated microscope, which allows automated image adquisition and analysis. Each well was divided in four stacks with a working distance of 0.2 μm. The first height was 7.6 μm and the last height was 8.2 μm. We selected three channels for analysis: Brightfield, Hoechst and Fluorescein. The images were captured using a 20× objective, long WD. Hoechst allows to identify cell nuclei (excitation = 360–400 nm, emission = 410–480 nm, exposure time = 100 ms) and Fluorescein to identify SA-β-Gal activity (excitation = 460–490 nm, emission = 500–550 nm, exposure time = 1800 ms). Brightfield images were captured by using exposure time = 20 ms.

2.9. Data analysis for chondrocyte senescence

SA-β-Gal data from the screening assay was analysed by using Harmony® Image Analysis Software. We calculated the average intensity of cytoplasmic fluorescein and number of nuclei in test samples, as well as in positive and negative controls. Then, we determined a threshold to define the maximum of senescence. For this, we subtracted twice the standard deviation from the intensity of cytoplasmic fluorescein was substracted two values from the standard deviation (mean – 2SD). We use the mean - 2SD value to select compounds from the Prestwick chemical library. We determined Z'factor, coefficient of variation (CV) values and signal-to-background (s/b) ratio for each plate [35]. Screening assay plate data was considered acceptable if $Z' \geq 0.5$ (Supplementary Fig. 1).

2.10. Autophagy screen

pBABE-puro mCherry-EGFP-LC3B plasmid was obtained from Addgene. mCherry-EGFP-LC3 retrovirus was produced as described previously [36]. HEK 293-T17 (ATCC®, cat# CRL-11268, RRID:CVCL_1926) cells were used to facilitate retroviral packaging. We employed FuGene Transfection Reagent, a nonliposomal mixture of lipids as a plasmid delivery method. After confirmation of transfection by microscopy, cells were sorted. Next, we selected the brightest clones by testing the expression of mCherry and GFP by flow cytometry. Finally, Operetta was used to evaluate the autophagic flux of selected clones by imaging. Stable clones were maintained in the presence of Puromycin (2.5 μg/ml). A Multidrop Combi Reagent Dispenser was used for seeding cells into 384-well plates (8000 cells/well) in DMEM media supplemented with 10% FCS, 1% P/S and 2.5 μg/ml Puromycin. Cells were incubated overnight at 37 °C and 5% CO_2. Echo®550 Acoustic Liquid Dispensing Technology was used to transfer compounds that were positive in the anti-senescence screen. The controls in this assay included DMEM supplemented with 2% FCS, IL-6 (20 ng/ml) and Chloroquine (30 μM). Once the cells adhered to the well, we removed the medium of the final plate and an automated JANUS workstation was employed to transfer 50 μl per well from interval plates to assay plates. Plates were incubated for 16 h at 37 °C in an atmosphere of 5% CO_2. After incubation, cells were fixed with PFA 4% for 10 min at 37 °C, washed with HBSS and then, the nuclei were stained with Hoechst (2.5 μg/ml) for 10 min at 37 °C. A Microplate Washer Robot and a Multidrop Combi Reagent Dispenser were used. We used a high-throughput method for quantifying autophagic flux. We employed the same HTS platform as in the SA-β-Gal assay. The images were captured using Operetta. Each well was divided into four stacks with a working distance of 0.2 μm. The first height was 7.6 μm and the last height was 8.2 μm. Cells were selected using four channels: Brightfield, Hoechst 33342, Fluorescein (EGFP), RFP (mCherry). The images were captured using a 20× objective, long WD as described in the senescence screen.

2.11. Data analysis of autophagic flux

Screening data were analysed using Harmony software. We calculated mCherry/EGFP Relative Spot Intensity with Harmony Analysis software. We obtained the mean and standard deviation of the positive and negative controls. We determined Z'factor, CV values and s/b (signal-to-background) ratio for each plate [35]. We use the (mean + 2SD) value to select compounds from the Prestwick chemical library. Screening assay plate data was considered acceptable if $Z' \geq 0.5$ (Supplementary Fig. 2).

2.12. Determination of senotherapeutic activity

Human chondrocytes (T/C28a2) were seeded (1×10^4 cells/well) in 96-well plates cultured for 24 h and then treated with IL-6 (20 ng/ml) and a PPARα agonists (Fenofibrate, CP775146, GW7647) at the indicated concentrations. Navitoclax (2.5 μM) and Rapamycin (10 μM) were used because of their senolytic and senomorphic effects, respectively. Following addition of the drugs, cells were incubated for 72 h. For fluorescence analysis of SA-β-Gal activity, we followed the same protocol as mentioned in *SA-β-Gal Activity Screening*. For quantitative analysis of total cell number (Hoechst staining) and number of senescent cells (C_{12}FDG staining), a laser-based scanning confocal imager (IN Cell Analyzer 6000, GE Healthcare) was used. An acquisition protocol was established using the Acquisition software v4.5, including parameters such as the plates and wells that were imaged, wavelengths, and exposure time. The acquired images were analysed using the Multi Target Analysis Module that allows the creation of various decision trees and the application of appropriate classification filters to different image stacks. All samples were analysed in duplicate with 3–5 fields per well and mean values and standard deviations being calculated accordingly.

2.13. Assessment of cell death

Annexin V apoptosis detection kit was used according to the manufacturer's instructions (Immunostep). Chondrocytes were labelled with Annexin V and Propidium iodide. For each condition, 10,000 events were collected and FACSCalibur and CellQuestPro software was used to analyse the data. Results were represented as percentage of Annexin-V positive cells and percentage of Propidium iodide positive cells.

2.14. Quantitative reverse transcription-polymerase chain reaction (qRT-PCR)

Total RNA was extracted from blood of Non-OA and Knee OA patients using Ribopure RNA purification kit and from human T/C28a2 chondrocytes using TRIZOL reagent. Then, 1.5 μg of RNA was used for complementary DNA (cDNA) synthesis using iScript cDNA synthesis kit and NZY First-Strand cDNA Synthesis kit for blood and cells, respectively. qRT-PCR was performed using Taqman Fast Advance Master Mix. Target gene expression was calculated using the comparative CT method (ΔΔCT) and normalized to an internal control gene 36B4 (qBASE+ qPCR analysis software). The following Taqman probes were used: Hs00797944 s1 MAP1LC3 FAM, Hs00231106 m1 FOXO1 FAM, Hs00355782 m1 CDKN1A FAM, Hs05332856 s1 NFκβ FAM, Hs00912671 m1 CPT1A FAM, Hs01074241 m1 ACOX1 FAM and Hs00947536 m1 PPARα FAM.

2.15. Safranin O staining

Cartilage explants from human normal ageing patients were employed to evaluate cartilage degradation in response to IL-1β. Serial sections (4 μm) were cut, stained with Safranin O– fast green to evaluate proteoglycan loss.

2.16. Nitric oxide assay

Griess reaction was used to quantify Nitric oxide (NO) production in the medium of primary human chondrocytes. An equal volume of Griess reagent and cellular supernatant (50:50 μl) were mixed and shaken for 10 min in the dark. Absorbance was measured at 570 nm on a microplate reader (Nanoquant Infinite M200).

2.17. Western blotting

Western blotting was performed with a chemiluminescence detection system. Cell lysates were obtained from OA and ageing primary human chondrocytes. Protein Sample preparation and Western Blotting was performed as described previously [37]. The membranes were incubated with primary antibodies against p21 (1:1000), p16 (1:1000), prpS6 (1:2000), LC3 (1:1000), NF-κB p65 (1:1000) and PPARα (1:1000) at 4 °C overnight. α-Tubulin antibody (1:5000) was incubated for 1 h at room temperature. Next, the membranes were incubated with horseradish peroxidase (HRP)-conjugated anti rabbit IgG for 1 h at RT. Membranes were washed 3 times with TBS-T and protein bands were detected using a chemiluminescence substrate and a detection system (Amersham Imager 600). The intensity of the bands was quantified by using ImageJ software.

2.18. Autophagy inhibition by transfection with PPARα small interference RNA

T/C28a2 human chondrocytes were transiently transfected with small interference RNA (siRNA) for PPARα, using Lipofectamine RNAiMAX transfection reagent according to the manufacturer's instructions. Silencer Cy-labelled negative Ctrl N.1 siRNA was employed as control.

2.19. Histological analyses

Human knee cartilage samples from normal ageing donors ($n = 3$) were fixed in 10% zinc-buffered formalin for 24 h. Knee joints from 6, 12, 18 and 30-month-old C57BL/6 J mice with spontaneous ageing-related OA (n = 3 per time point) and from C57BL/6 J mice with OA induced by transection of the medial meniscotibial ligament and the medial collateral ligament (MMTL+MCL) (sham surgery and 10 weeks after surgery; n = 3) were fixed in 10% zinc-buffered formalin for 24 h and decalcified in TBD-2 for 48 h. Sections were stained with Safranin O–fast green. Histological scoring of OA-like changes on the medial femoral condyle and tibial plateau from mice was performed using the Osteoarthritis Research Society International (OARSI) scoring system (score range 0 to 6) [38]. Paraffin sections from mouse models were provided from Dr. Martin Lotz at the Scripps Research, La Jolla, CA, USA.

2.20. Immunohistochemistry

Human cartilage and mouse knee joint sections were deparaffinized, washed, and blocked with 10% goat serum. Primary antibody against PPARα (1:500) was applied and incubated overnight at 4 °C, followed by ImmPRESS reagents. The signal was developed with Diaminobenzidine-Peroxidase substrate Kit. The number of PPARα-positive cells was quantified.

2.21. Quantification of positive chondrocytes in human cartilage and mouse knee joint sections

In human cartilage, 3 pictures per section were taken under 10× magnification. In mouse knee joints from spontaneous ageing-related OA model and surgically induced OA, 3 pictures were taken under 10× magnification, showing the center of the femoral condyle that is not covered by the menisci as well as the medial and lateral femoral condyles. Then, the total number of PPARα-positive cells was counted in each section [39].

2.22. Statistical analysis

To test for normal distribution of the data, we used the Kolmogorov-Smirnov test. In general, the data sets followed a normal distribution. Statistically significant differences between 2 groups were determined by Student's *t*-test, while differences between multiple groups were determined analyzing variance (ANOVA) in conjunction with Tukey's multiple comparison. The data analysis and statistical inference was performed by using Prism 6.0 software. The results are reported as the mean ± SEM. p values $<.05$ were considered significant.

2.23. Analysis of knee osteoarthritis patients treated with fibrates from Osteoarthritis Initiative (OAI) Cohort

For the present study, we used longitudinal data obtained from the multicenter, longitudinal, prospective observational study of knee OA, Osteoarthritis Initiative (OAI). The OAI data are publicly available at https://oai.nih.gov. Specific datasets used were: “MIF00”, “MIF01”, “MIF03”, “MIF05” (release versions 0.2.2, 1.2.1, 3.2.1, and 5.2.1, respectively); “AllClinical00”, “AllClinical01”, “AllClinical03”, “AllClinical05” (release versions 0.2.3, 1.2.2, 3.2.1, and 5.2.1, respectively); “Enrollees00 (release version 25)”; “Outcomes99” (release version 10).

The detailed information about the OAI protocol can be found at the osteoarthritis initiative protocol for the cohort study, from http://data-archive.nimh.nih.gov/binaries/content/documents/ndacms/resources/oai/oai-study protocol/oai-study-protocol/ndacms%3Aresource. The OAI cohort consists of a progression subcohort (patients with symptomatic tibiofemoral knee OA, $n = 1390$), an incidence subcohort (subjects with increased risk of OA, $n = 3284$) and a reference control subcohort ($n = 122$). In this analysis we used the longitudinal data from both the progression and incidence subcohorts. The main inclusion criteria were the following: age between 45 and 79 years for both subcohorts, symptomatic tibiofemoral knee OA for the progression subcohort, and the presence of established or putative risk factors for incident knee OA for the incidence subcohort. The OAI participants were recruited and enrolled between February 2004 and May 2006 at four recruitment centres in the United States. This study was approved by institutional review board committees from each recruitment centre. Before entering the study, all participants provided written informed consent. The prespecified sample size was 5000 participants (4000 in the incidence subcohort, 800 in the progression subcohort). It was expected that this sample size would provide an adequate number of knees with incident and worsening OA-related structural and clinical changes in order to achieve the primary aims of the OAI study.

2.23.1. Clinical measures

Height was measured in millimetres using a calibrated, wall-mounted stadiometer. The measurement was performed twice with the subject in light clothing, without shoes, and during inspiration. Body weight was measured in kilograms with a calibrated, standard balance beam scale. The measurement was performed twice with the subject in light clothing without shoes, heavy jewellery or wallets. Body mass index (BMI) was calculated based on weight (in kg) divided by height (in cm) squared. Prior knee surgery was evaluated using interview. Self-reported physical activity was measured using the Physical

Activity Scale for the Elderly (PASE) [40]. To evaluate the severity of OA symptoms, the self-reported Western Ontario McMaster Osteoarthritis Index (WOMAC) (5 point Likert scale) for addressing pain, function, and stiffness was used [41]. The possible range for pain was 0–20, for physical function was 0–68, and for stiffness was 0–8. In OAI, WOMAC subscores are reported separately for each knee. For the analyses, we used the highest from the left and right sided scores for the WOMAC subcategories. The outcomes were assessed at baseline and annually until year 3. The WOMAC scores after joint replacement were coded as missing values.

To acquire information about the use of fibrates, a medication inventory method was used. In this method the participants bring in all of the medications they are currently taking, and the brand name, generic name or active ingredients are recorded and matched to an entry in

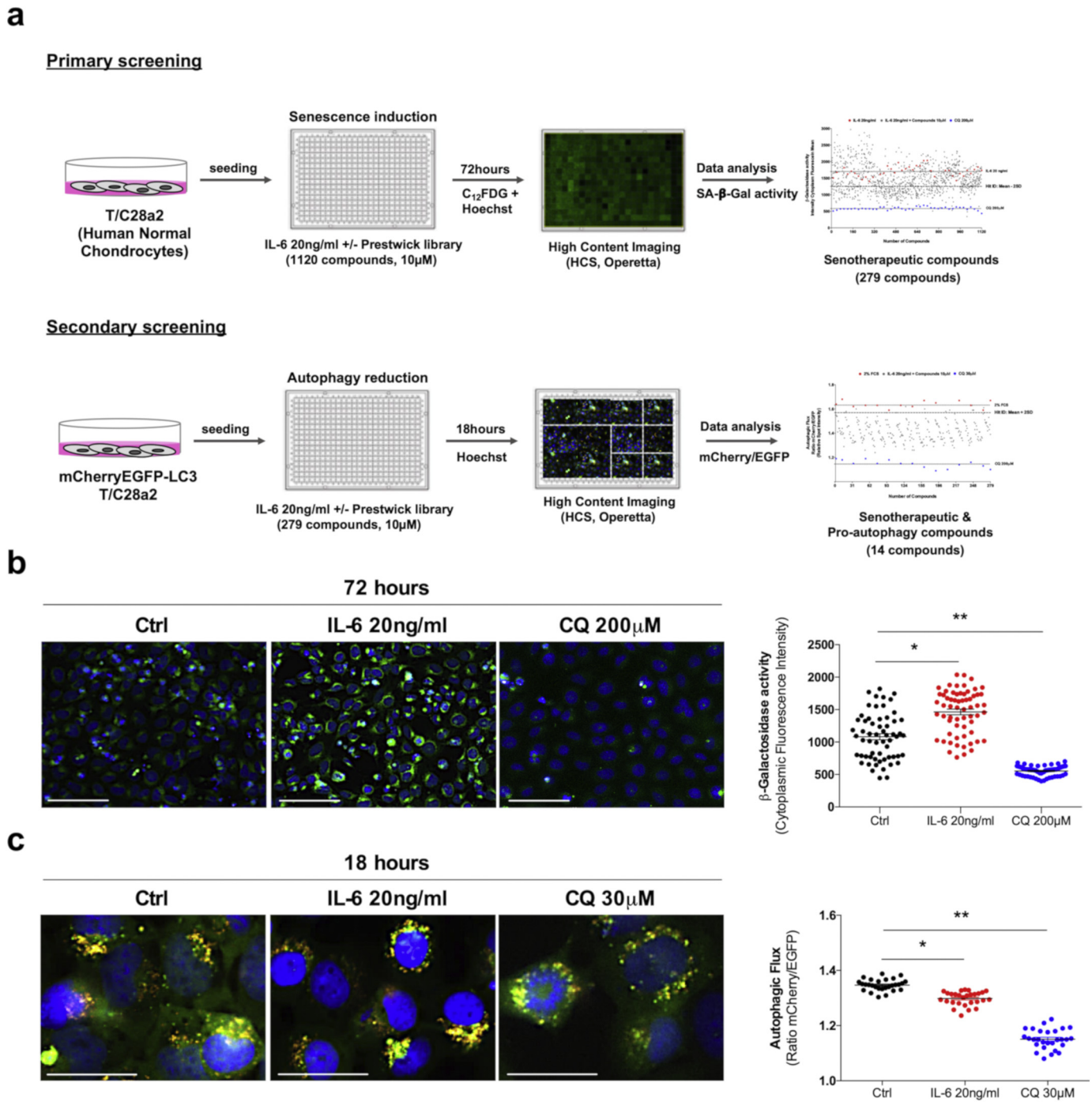

Fig. 1. Cell-based imaging screening to identify senescence and autophagy modulators. a. Schematic imaging screening development. Primary screening was performed in T/C28a2 human chondrocytes treated with IL-6 (20 ng/ml) +/− Prestwick Chemical Library (1120 compounds, 10 μM) for 72 h in a 384 well plate. Hoechst 33342 (1 μM) was employed for 10 min for nuclei staining. Then, chondrocyte senescence was determined with C_{12}FDG to quantify senescence-associated β-Galactosidase (SA-β-Gal) activity by using a High Content Imaging System (HCIS). Secondary screening was performed in an autophagy reporter cell line in human chondrocytes (mCherryEGFPLC3 T/C28a2) treated with IL-6 (20 ng/ml) +/− Prestwick Chemical Library (279 compounds, 10 μM) for 18 h in a 384 well plate. Hoechst 33342 (1 μM) was employed for 10 min for nuclei staining b. IL-6 (20 ng/ml) induced chondrocyte senescence at 72 h. Cellular senescence was determined with the Galactosidase susbtrate, C_{12}FDG by HCIS. Chloroquine (CQ, 200 μM) was employed as SA-β-Gal inhibitor. Scale bar, 100 μm. SA-β-Gal activity was represented by the intensity of the cytoplasm fluorescein. Values are mean ± SEM of 60 well/condition, $^{*}p < .0001$, $^{**}p < .0001$ *vs. Ctrl*, two-tailed unpaired Student's *t*-test. c. IL-6 (20 ng/ml) reduced autophagic flux at 18 h. Chloroquine (CQ, 30 μM) was employed as autophagic flux inhibitor. Scale bar, 50 μm. Autophagic flux was represented by the ratio between mCherry/EGFP. Values are mean ± SEM of 28 well/condition, $^{*}p < .0001$, $^{**}p < .0001$ *vs. Ctrl*, two-tailed unpaired Student's *t*-test.

an online medication dictionary [42]. Fibrate users were defined as those with at least one recorded use during first three years of the study, excluding baseline use (a "new-user" design). We considered participants to be users regardless of consistency of fibrate use and its duration, thus mimicking intent-to-treat analysis in randomized controlled studies.

2.23.2. Statistical analysis

The genetic matching method was used to match fibrate users with non-users. Genetic matching is a multivariable matching approach making the distribution of baseline characteristics in "treatment" and "control" groups as similar as possible. Genetic matching uses an automated evolutionary search algorithm to determine the weight each covariate is given. This method combines multivariate matching on the covariates and propensity score-matching that allows to optimize covariate balance between matched samples. Compared with other matching methods, genetic matching has been found to improve covariate balance and reduce bias [43]. We used one-to one matching with replacement as it was shown to lead to less bias [44]. The following potential confounding variables were used for the matching: demographic characteristics, body mass index, prior knee surgery, baseline outcome measures, and PASE. After all matches were done, differences between the two groups were compared by standardized differences, ≥ 0.1 was defined as meaningful disbalance [45]. After matching was performed, generalized estimating equations (GEE) were used to model the relationship between outcomes measured over time and fibrate use. For the assessment of changes in outcome measures over time, we used the user*time interaction term. A β-coefficient for this interaction term indicates yearly change in the outcome parameter assuming linear development over time. The GEE models were fitted using robust

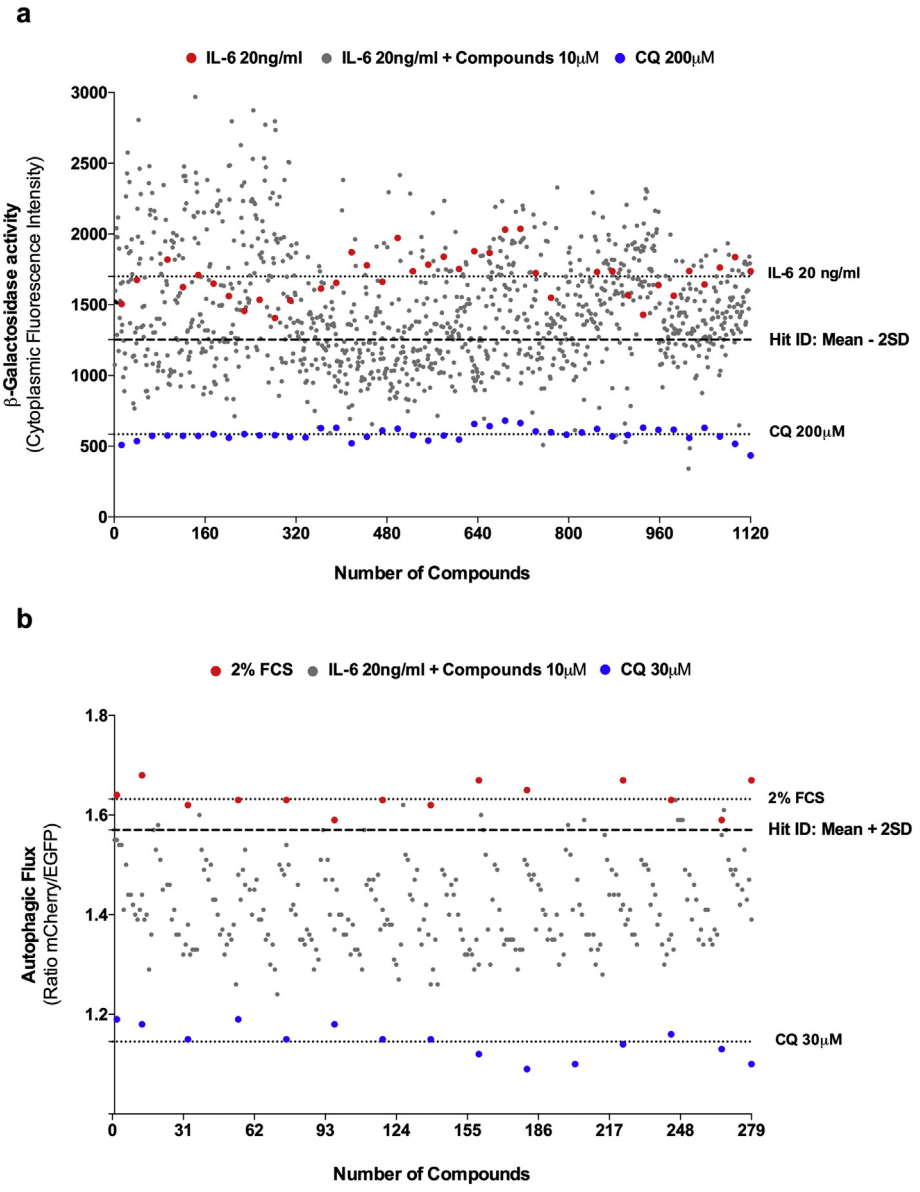

Fig. 2. Identification of senescence and autophagy modulators. a. Primary screening was performed in T/C28a2 human chondrocytes treated with IL-6 (20 ng/ml) +/− Prestwick Chemical Library 10 μM (1120 compounds) at 72 h. CQ (200 μM) for 30 min was employed as negative control of SA-β-Gal activity. SA-β-Gal activity was determined by C_{12}FDG and represented by mean of cytoplasmic fluorescein intensity. 279 compounds were identified as senotherapeutics. Compounds were considered hits by *mean - 2SD* on average *Z'factor* of *0.53*. b. Secondary screening in mCherryEGFPLC3 T/C28a2 human chondrocytes treated with IL-6 (20 ng/ml) +/− of Prestwick Chemical Library 10 μM (279 compounds) at 18 h. CQ (30 μM) was employed as negative control for autophagic flux. Autophagic flux was determined by the ratio mCherry/EGFP. 14 compounds were identified as senotherapeutics and autophagy modulators. Compounds were considered hits by *mean + 2SD* on average *Z'factor* of *0.58*.

Table 1
Identified compounds with senotherapeutic and pro-autophagy activity.

Compounds	β-Gal activity	Cell number	Autophagic flux	Target
Bupivacaine hydrochloride	1142	865	1.60	Sodium ion channels
Minoxidil	1185	950	1.59	Potassium channels
Fenofibrate	1234	997	1.57	Peroxisome Proliferator Receptor α
Pentolinium bitartrate	1162	964	1.59	Unknown
Tomatine	1142	970	1.57	Unknown
Benzydamine hydrochloride	1196	1016	1.57	Cyclooxygenase
Ciproheptadine hydrochloride	1031	914	1.6	Histamine H1 and Serotonin receptors
Lomefloxacin hydrochloride	1155	1046	1.58	DNA replication
Flutamide	1091	995	1.57	Androgen receptor
Digitoxigenin	1382	1262	1.59	Na,K ATPase
Guanethidine sulfate	1101	1030	1.58	Adrenergic system
Antipyrine	997	1046	1.61	Prostaglandin G/H synthase 1 and 2
Astemizole	712	770	1.63	Histamine H1 receptor
Pherphenazine	878	985	1.62	Dopamine D2 receptor

standard errors computed by a "sandwich" estimator. An exchangeable correlation structure was used to correct for the correlation between repeated measurements. Although selection of proper correlation structure is the assumption in GEE models, the method is robust against violation of this assumption. GEE allows for not using imputation methods for the missing data, because the participants with missing data are not excluded from the analysis [46]. Genetic matching was performed using "Matchit" package for R (version 3.0.2) [47]. GEE analyses were done with "gee" package for R (version 4.13–19) [48]. All statistical analyses were performed using R software (version 3.5.1).

3. Results

3.1. Identification of senescence and autophagy modulators

A cell-based imaging assay in human chondrocytes was used to identify compounds that modulate senescence and autophagy as novel OA disease-modifying therapeutics. Chondrocytes were treated simultaneously with IL-6 and compounds from the Prestwick Chemical library. To quantify senescence, fluorescent SA-β-Gal activity was analysed using the C_{12}FDG substrate and the ratio of fluorescent signal

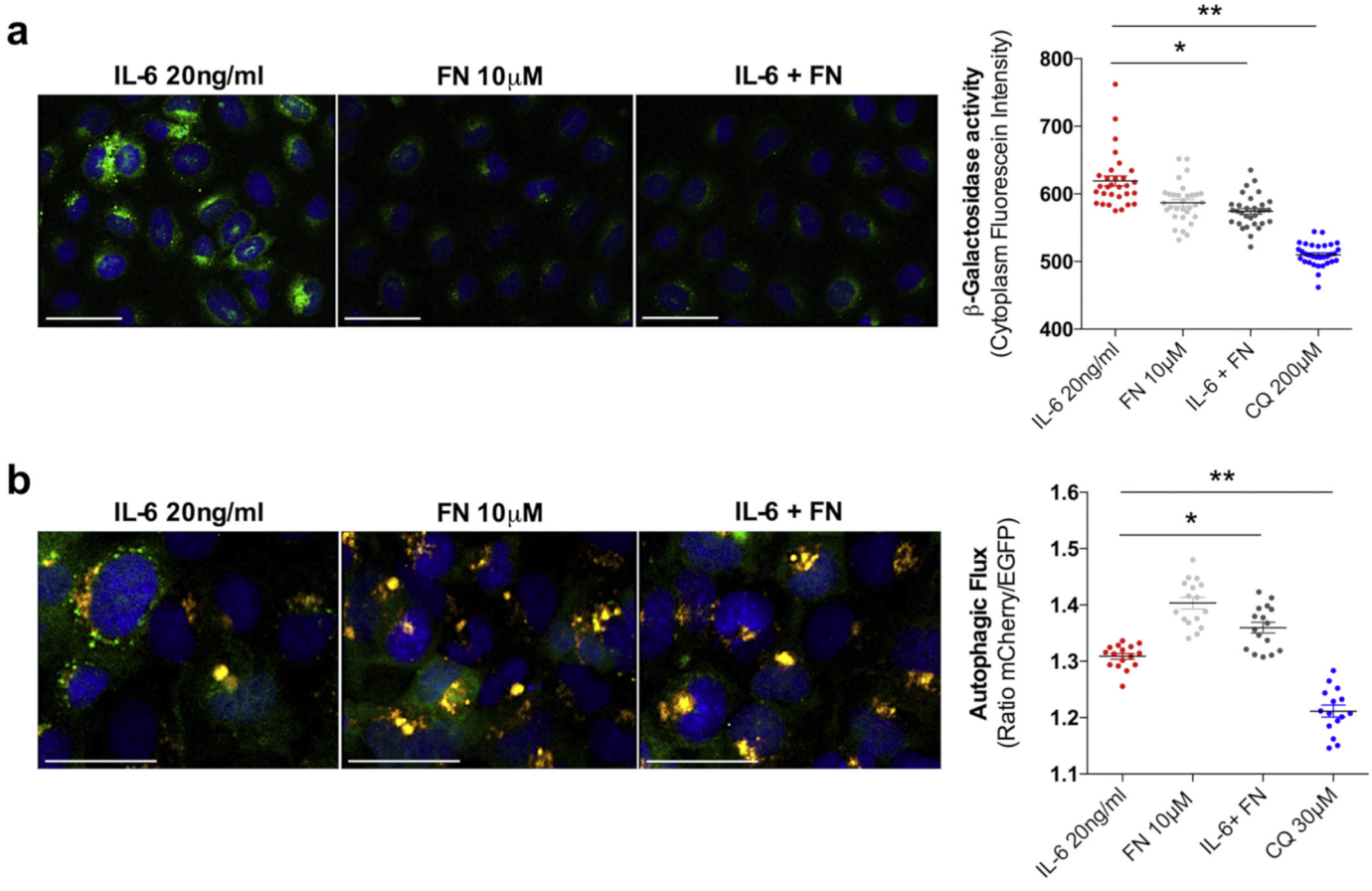

Fig. 3. Fenofibrate, a PPARα agonist, reduces chondrocyte senescence and induces autophagic flux. a. T/C28a2 human chondrocytes were treated with IL-6 (20 ng/ml), or FN (10 μM), or in combination for 72 h in a 384 well plate. CQ (200 μM) was employed as inhibitor of SA-β-Gal activity. Scale bar, 100 μm. Values are mean ± SEM of 30 well/condition, $^{*}p < .0001$, $^{**}p < .0001$ *vs. IL-6*, two-tailed unpaired Student's *t*-test. b. mCherry-EGFPLC3 T/C28a2 human chondrocytes were treated with IL-6 (20 ng/ml), or FN (10 μM), or in combination for 18 h in a 384 well plate. CQ (200 μM) was employed as inhibitor of autophagic flux. Scale bar, 50 μm. Values are mean ± SEM of 16 well/condition, $^{*}p < .0001$, $^{**}p < .0001$ *vs. IL-6*, two-tailed unpaired Student's *t*-test.

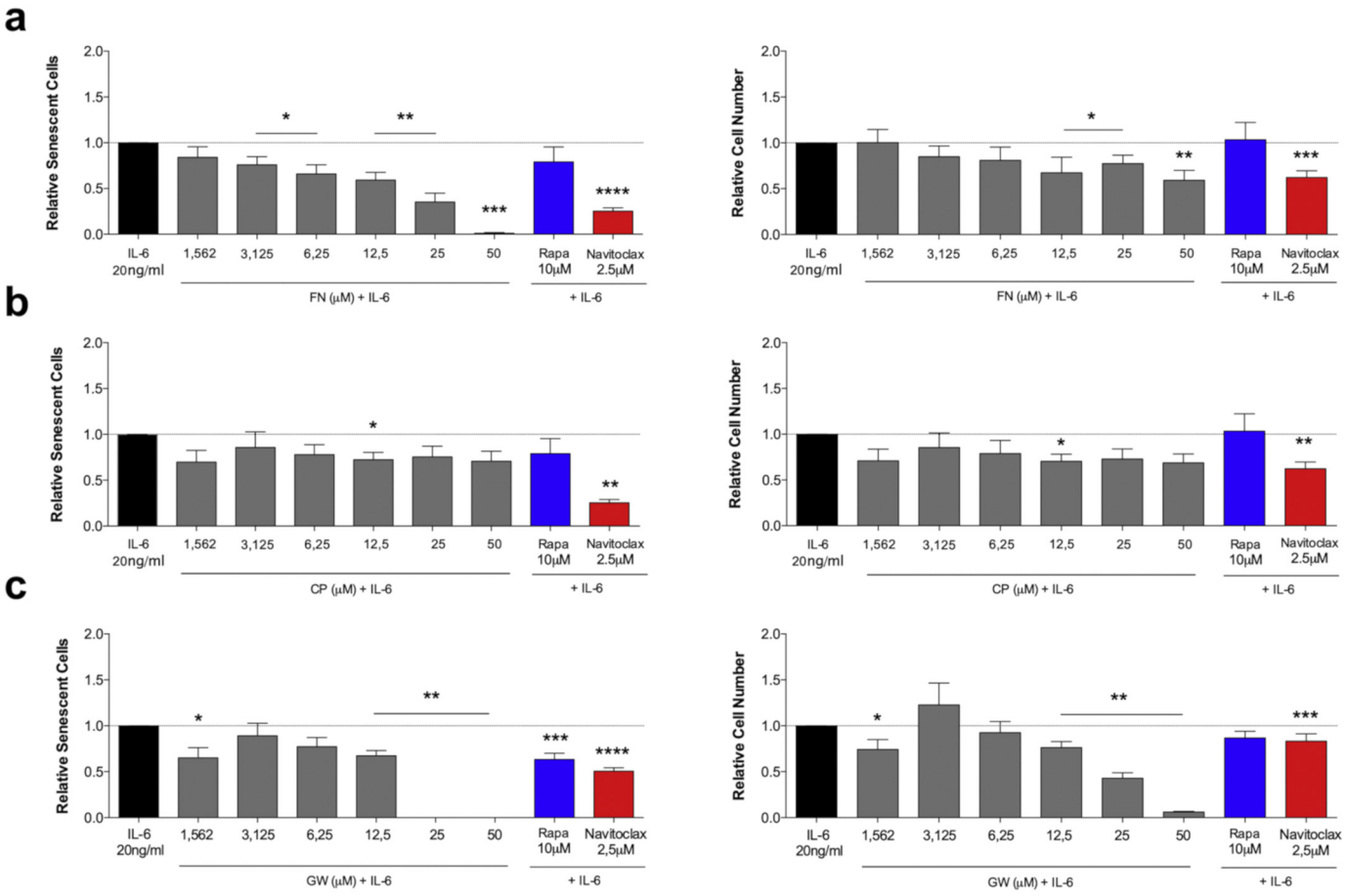
a
Relative Senescent Cells
Relative Cell Number
IL-6 20ng/ml
1,562
3,125
6,25
12,5
25
50
Rapa 10μM
Navitoclax 2.5μM
FN (μM) + IL-6
+ IL-6
b
CP (μM) + IL-6
c
Navitoclax 2,5μM
GW (μM) + IL-6

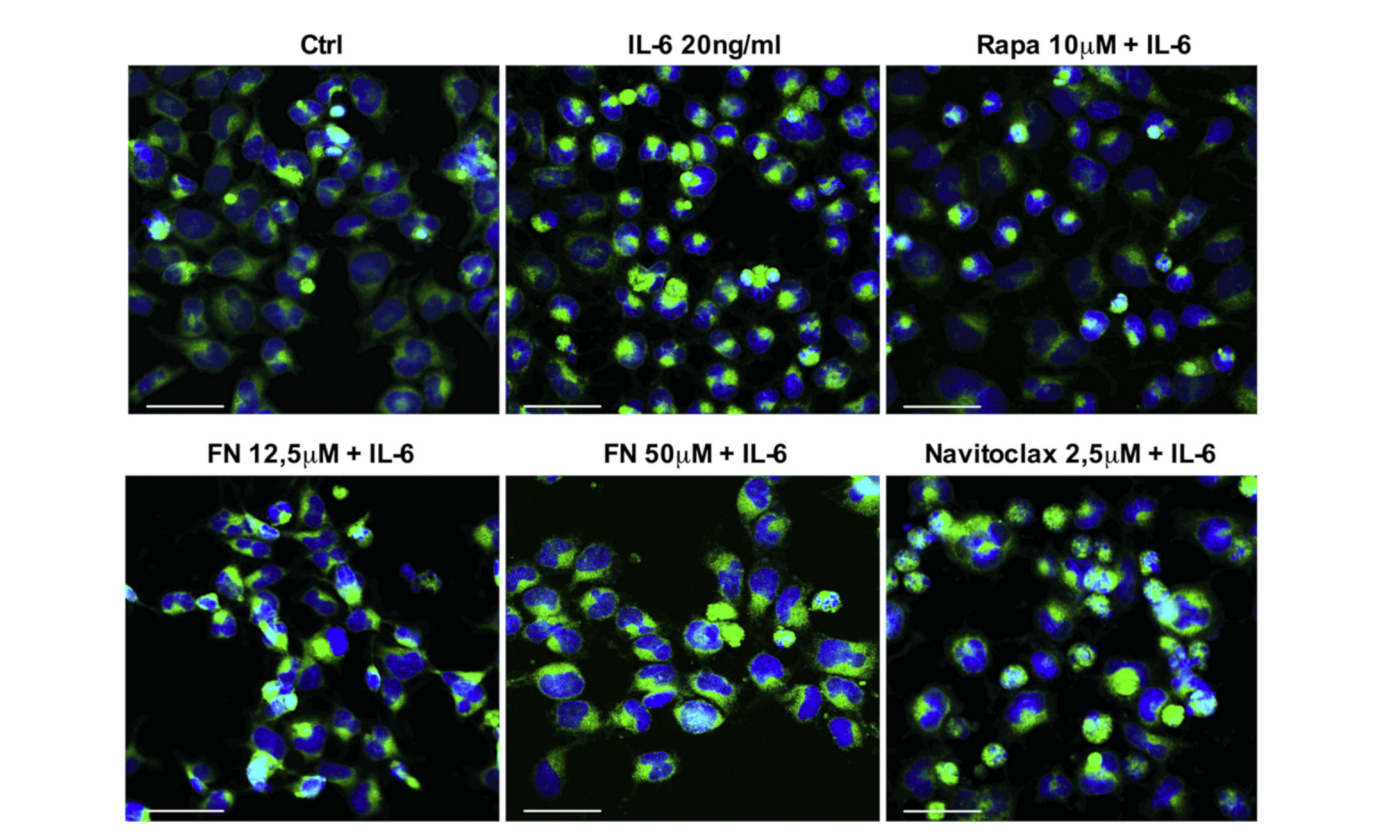
d
Ctrl
IL-6 20ng/ml
Rapa 10μM + IL-6
FN 12,5μM + IL-6
FN 50μM + IL-6
Navitoclax 2,5μM + IL-6

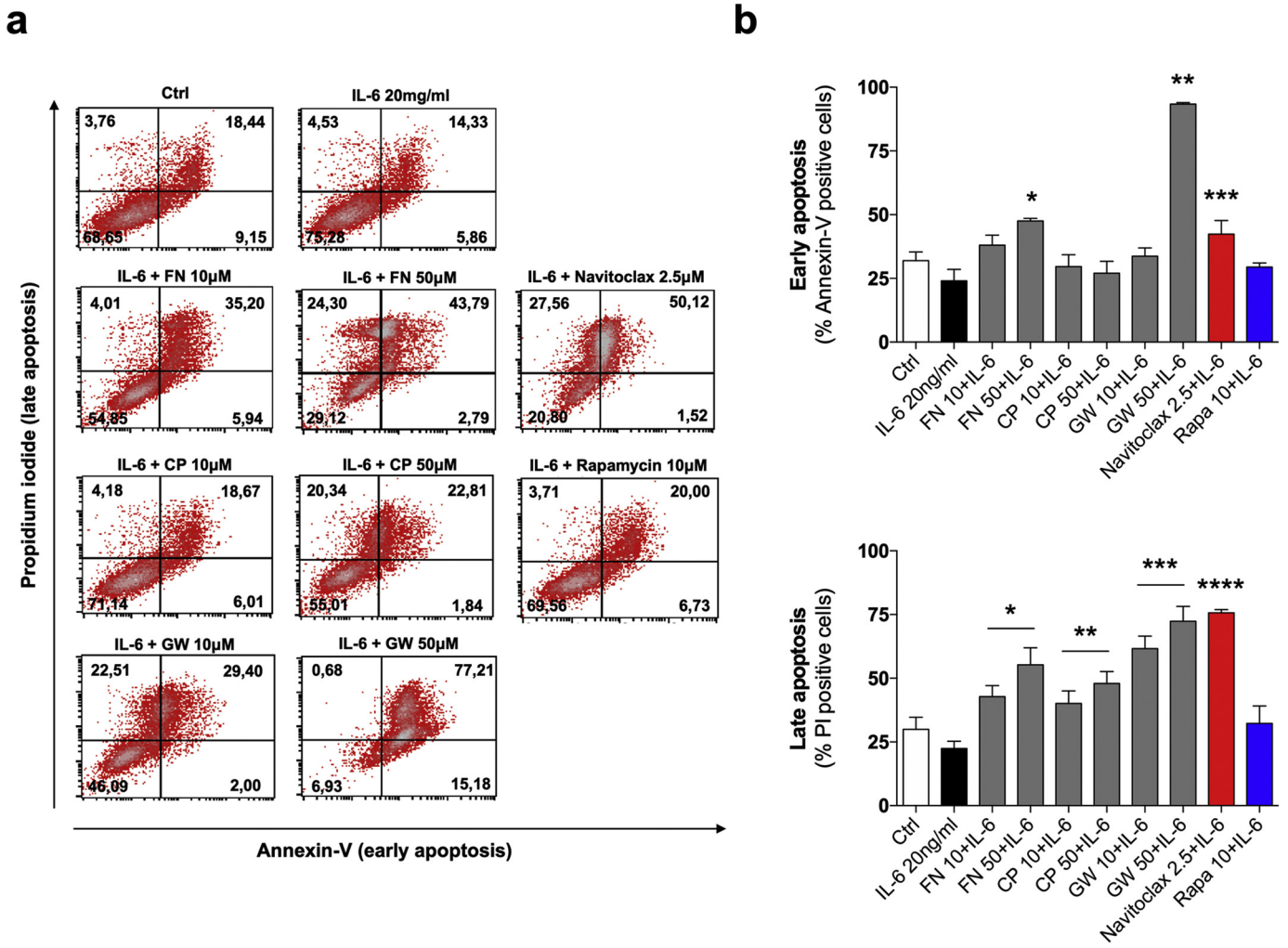

Fig. 5. FN selectively kill senescent chondrocytes through inducing cell death by apoptosis. a. Flow cytometry determination of early apoptosis by Annexin-V staining, and late apoptosis by propidium iodide (PI) staining in T/C28a2 human chondrocytes treated with IL-6 (20 ng/ml), or in combination with FN, CP and GW (10, 50 μM), Rapa (10 μM), or with Navitoclax (2.5 μM) for 72 h in a 12 well plate. b. Quantitative analysis of chondrocyte death by Annexin-V and PI staining in human chondrocytes. Values are mean ± SEM of three independent observations. Early apoptosis: *$p < .01$, **$p < .0001$, ***$p < .05$ *vs. IL-6*; Late apoptosis: *$p < .05$, **$p < .05$, ***$p < .01$, *and* ****$p < .0001$ *vs. IL-6*, two-tailed unpaired Student's *t*-test.

intensity in LC3 punctae was used as a marker of LC3-mediated autophagic flux (Fig. 1a). In this system, IL-6 induced a significant increase in both the percentage of cells positive for in SA-β-Gal activity at 72 h (Fig. 1b) and overall SA-β-Gal activity. Similarly, IL-6 induced a significant decrease in autophagic flux as well as the percent of cells positive for autophagy at 18 h (Fig. 1c). Chloroquine (CQ), an intracellular β-Gal and autophagic flux inhibitor, was employed as a negative control. In addition, p21, an important senescence marker [49] and phosphoribosomal S6 (prbS6), a direct target of the mammalian target of rapamycin (mTOR) [50], were significantly increased after IL-6 stimulation (Supplementary Fig. 3).

Results showed that 279 compounds from the Prestwick library decreased IL-6 induced senescence (Fig. 2a). From this set of 279, 14 compounds also increased autophagic flux and were selected as dual senescence and autophagy modulators for confirmatory studies (Fig. 2b). The compounds identified primarily targeted ion channels and hormone receptors related to metabolism (Table 1). Peroxisome proliferator-activated receptor alpha (PPARα), a therapeutic target for lipid metabolism dysfunction [32] was considered relevant for chondrocyte homeostasis so PPARα modulators were selected for further studies. Fenofibrate (FN), a PPARα agonist significantly reduced SA-β-Gal activity in IL-6 treated chondrocytes at 72 h (Fig. 3a) and this was accompanied by an increase in autophagic flux at 18 h (Fig. 3b), confirming its senotherapeutic and autophagy promoting activity.

3.2. PPARα agonists function as senolytics to selectively kill senescent chondrocytes through cell death by apoptosis

To characterize the senotherapeutic activity of FN and other selective PPARα agonists, such as CP775146 and GW7647, the agonists

Fig. 4. PPARα agonists are senolytics in human chondrocytes. a. T/C28a2 human chondrocytes were treated with IL-6 (20 ng/ml) in combination with FN (1,582 – 50 μM), Rapa (10 μM), or Navitoclax (2.5 μM) for 72 h in a 96 well plate. Relative senescence cells: values are mean ± SEM of 4 well/condition, *$p < 0.05$, **$p < 0.01$, ***$p < 0.0001$ *and* ****$p < 0.0001$ *vs. IL-6*. Relative cell number: values are mean ± SEM of 4 well/condition, *$p < 0.05$, **$p < 0.01$ *and* ***$p < 0.01$ *vs. IL-6*, two-tailed unpaired Student's t-test. **b.** T/C28a2 human chondrocytes were treated with IL-6 (20 ng/ml) in combination with CP (1,582 – 50 μM), Rapa (10 μM), or Navitoclax (2.5 μM) for 72 h in a 96 well plate. Relative senescence cells: values are mean ± SEM of 4 well/condition, *$p < 0.01$, **$p < 0.0001$ *vs. IL-6*. Relative cell number: values are mean ± SEM of 4 well/condition *$p < 0.01$, **$p < 0.01$ *vs. IL-6*, two-tailed unpaired Student's t-test. **c.** T/C28a2 human chondrocytes were treated with IL-6 (20 ng/ml) in combination with GW (1,582 – 50 μM), Rapa (10 μM), or Navitoclax (2.5 μM) for 72 h in a 96 well plate. Relative senescence cells: values are mean ± SEM of 4 well/condition, *$p < 0.05$, **$p < 0.001$, ***$p < 0.01$ *and* ****$p < 0.0001$ *vs. IL-6*. Relative cell number: values are mean ± SEM of 4 well/condition, *$p < 0.05$, **$p < 0.001$ *and* ***$p < 0.05$ *vs. IL-6*, two-tailed unpaired Student's t-test. **d.** Representative images of SA-β-Gal activity from T/C28a2 human chondrocytes treated with FN in response to IL-6 treatment. Scale bar, 100 μm.

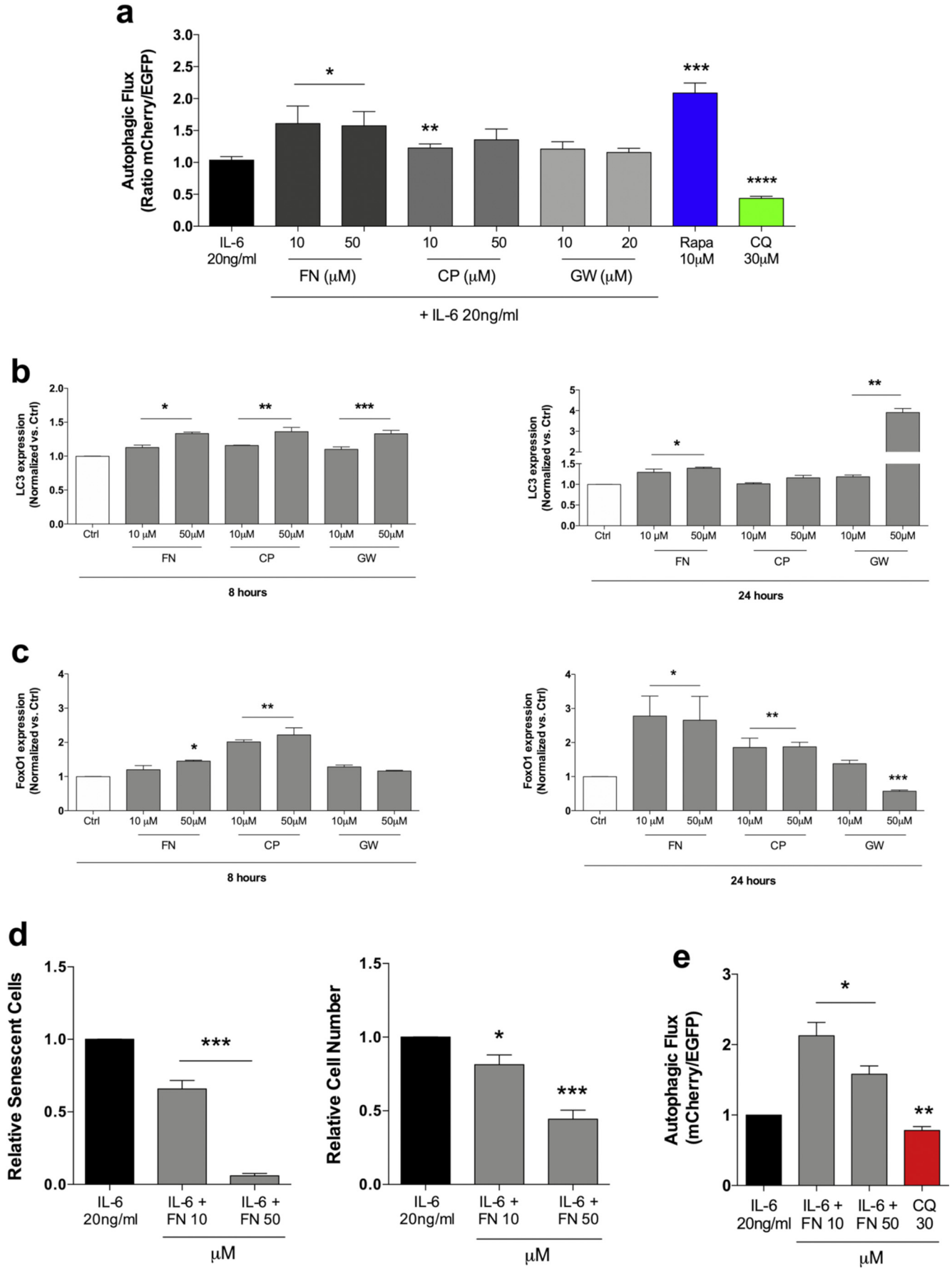
a
Autophagic Flux (Ratio mCherry/EGFP)
IL-6 20ng/ml
10
50
10
50
10
20
Rapa 10μM
CQ 30μM
FN (μM)
CP (μM)
GW (μM)
+ IL-6 20ng/ml
b
LC3 expression (Normalized vs. Ctrl)
Ctrl
10 μM
50μM
FN
CP
GW
8 hours
24 hours
c
FoxO1 expression (Normalized vs. Ctrl)
d
Relative Senescent Cells
Relative Cell Number
IL-6 20ng/ml
IL-6 + FN 10
IL-6 + FN 50
μM
e
Autophagic Flux (mCherry/EGFP)
CQ 30

(1.5–50 μM) were added to chondrocytes treated with IL-6 (20 ng/ml) for 72 h. The PPARα agonists showed senolytic activity in human chondrocytes by reducing both the number of senescent cells and total number of cells. FN showed a dose-dependent senolytic effect (Fig. 4a), GW7647 was toxic at 50 μM (Fig. 4b) and CP775146 was senolytic only at 12.5 μM (Fig. 4c). Navitoclax and Rapamycin (Rapa) were employed as positive control for senolytic and senomorphic activity, respectively.

To investigate how senescent cells were eliminated by PPARα agonists, chondrocyte death was determined by evaluating early and late apoptosis, using annexin-V and propidium iodide (PI), respectively (Fig. 5a). Quantification of apoptosis demonstrated that PPARα agonists (10 and 50 μM) selectively eliminated senescenct cells by increasing apoptosis following IL-6-mediated induction of senescence (Fig. 5b). FN showed similar effects to navitoclax (a reference control for senolytic activity), while the senomorphic drug rapamycin did not increase apoptosis. These results suggest that the senolytic activity of FN in human chondrocytes is associated with selective induction of apoptosis.

Moreover, to evaluate the senolytic effect of PPARα activation, senescent human IMR90 lung fibroblasts and DNA repair deficient *Ercc1*$^{-/-}$ MEFs fibroblasts were employed [28,51]. The results showed that PPARα agonists act as senolytics in both models, indicating the potential senotherapeutic effect of activating lipid metabolism in multiple senescent cell types (Supplementary Fig. 4 and Supplementary Fig. 5).

3.3. Homeostasis markers are positively regulated by PPARα agonists

To determine the effects of PPARα modulators on cellular homeostasis mechanisms such as autophagy and FoxO signalling pathway, human chondrocytes were treated with PPARα agonists (10 and 50 μM) following exposure to IL-6. Only FN increased autophagic flux at both concentrations while the other PPARα agonists showed lower and mostly non-significant effects. Rapamycin and chloroquine (CQ) showed the expected effects as positive and negative controls for autophagic flux (Fig. 6a). In addition, PPARα agonists also increased *LC3* and *FoxO1* gene expression at 8 and 24 h (Fig. 6 b, c). Taken together, these results demonstrate that FN regulates homeostasis in human chondrocytes as both a senolytic and autophagy modulating compound (Fig. 6d).

3.4. FN protects against cartilage degradation and regulates senescence, autophagy and inflammation

Treatment with FN reduced proteoglycan loss in cartilage explants and protected against cartilage degradation in response to IL-1β treatment (Fig. 7a). This protective role was correlated with a reduction of nitric oxide (NO) production (Fig. 7b). Moreover, FN treatment did not induce cell death in primary non-senescent human chondrocytes (Supplementary Fig. 6).

Human OA and ageing primary chondrocytes were employed to further investigate the influence of FN on senescence, autophagy, inflammation and cartilage degradation. The levels of expression of the senescence markers *p21* and *p16*, the key autophagy regulator LC3 and the p65/RelA subunit of NF-κB, a key regulator of SASP, were evaluated as well as the extent of phosphorylation of pS6 as a marker for mTOR activity. In OA chondrocytes, FN reduced expression of *p21 and* the NF-κB p65 subunit *RELA* (Fig. 7c) and reduced phosphor-S6. In ageing chondrocytes FN, reduced expression of *p16, p21 and NFκB/RELA* and increased expression of *LC3* while reducing the level of phospho-S6 (Fig. 7d). This regulation of senescence and autophagy markers in the chondrocyte cultures is likely conferred through the deletion of senescent chondrocytes. Remarkably, genetic deletion of PPARα promoted senescence and SASP/inflammation by increasing *p21* and NF-κB/RELA expression levels respectively as well as increased *LC3* and reduced *FOXO1* expression (Fig. 7e-i). These data are consistent with FN treatment inducing the selective elimination of senescent cells and favorably modulating inflammatory and metabolic responses involved in OA pathogenesis.

3.5. FN increases PPARα expression and regulates the β-oxidation transcriptional program in human chondrocytes

PPARα regulates fatty acid (FA) β-oxidation and is involved in regulation of energy homeostasis [52]. PPARα also appears to auto-regulate its own expression. Thus, we examined if FN regulates PPARα in human chondrocytes. FN treatment increased PPARα expression at both gene and protein level (Fig. 8a, b) and that PPARα agonists regulated FA β-oxidation genes in human chondrocytes (Fig. 8c, d).

3.6. PPARα is downregulated in mouse models of ageing and OA

The expression pattern of PPARα in cartilage with ageing and OA was investigated in natural ageing and in a surgically-induced OA model in mice. The number of PPARα-positive chondrocytes in knee cartilage significantly decreased with ageing, with only a minimal percentage of the cells positive for PPARα at 30 months (Fig. 9a). In the surgical OA model, 10 weeks after transection of the medial meniscotibial ligament and the medial collateral ligament (MMTL+MCL), PPARα-positive cells were also significantly reduced (Fig. 9b).

3.7. PPARα is reduced in OA patients and its pharmacological activation improved their clinical conditions

The relevance and potential translation of this mechanism was explored by analyzing human cohorts of OA patients. To invEstigate the role of PPARα as a potential biomarker of OA, blood from the PROspective Osteoarthritis Cohort of A Coruña (PROCOAC) and human cartilage from non-OA and knee OA patients were employed. Levels of PPARα were lower in OA patients compared to non-OA controls (Fig. 10a). In addition, immunohistochemical analysis of cartilage showed that PPARα was mainly expressed in the superficial zone in non-OA cartilage with decreased expression in OA grade III-VI patients. Moreover, in OA cartilage, PPARα positive cells were present only in the chondrocyte clusters (Fig. 10b, c).

The potential efficacy of PPARα agonists was also evaluated using the Osteoarthritis Initiative (OAI) Cohort. In this cohort, there were 35 fibrate users and 3322 participants not taking fibrates in the selected sample (Supplementary Fig. 7). Using a genetic matching, 35 fibrate users were matched to 35 participants in the control group. After matching, all standardized differences of means decreased to <0.05, indicating that the matched groups had <5% of standard deviation difference in the corresponding variables. Therefore, it was considered that covariates were well balanced between groups (Supplementary Table 1). From the total of 35 fibrate users, twenty-four users (68.6%)

Fig. 6. PPARα agonists modulate key homeostasis markers in human chondrocytes. a. mCherry-EGFPLC3 T/C28a2 human chondrocytes were treated with IL-6 (20 ng/ml) alone or in combination with PPARα agonists FN, CP and GW (10, 50 μM) for 18 h in a 96 well plate. Rapa (10 μM) and CQ (30 μM) were employed as activator and inhibitor of autophagic flux, respectively. Values are mean ± SEM of 6 independent observations, $^{*}p < 0.05$, $^{**}p < 0.05$, $^{***}p < 0.0001$ and $^{****}p < 0.0001$ *vs. IL-6*, two-tailed unpaired Student's t-test. **b.** Relative expression of LC3 in T/C28a2 human chondrocytes untreated or treated with FN, CP and GW (10, 50 μM) for 8 and 24 h. Values are mean ± SEM of 3 independent observations (8 h: $^{*}p < 0.01$, $^{**}p < 0.0001$, $^{***}p < 0.0001$ *vs. IL-6*; 24 h: $^{*}p < 0.05$, $^{**}p < 0.0001$ *vs. IL-6*, two-tailed unpaired Student's t-test). **c.** Relative expression of FoxO1 in T/C28a2 human chondrocytes untreated or treated with FN, CP and GW (10, 50 μM) for 8 and 24 h. Values are mean ± SEM of 3 independent observations (8 h: $^{*}p < 0.0001$, $^{**}p < 0.0001$ *vs. IL-6*, 24 h: $^{*}p < 0.05$, $^{**}p < 0.05$, $^{***}p < 0.01$ *vs. IL-6*), two-tailed unpaired Student's t-test. **d.** Relative senescence cells: values are mean ± SEM of 16 well/condition, $^{***}p < 0.0001$ *vs. IL-6*. Relative cell number: values are mean ± SEM of 16 well/condition, $^{*}p < 0.05$ and $^{***}p < 0.01$ *vs. IL-6*, two-tailed unpaired Student's t-test. **e.** Determination of autophagic flux. Values are mean ± SEM of 16 well/condition, $^{*}p < 0.0001$, $^{**}p < 0.0001$ *vs. IL-6*, two-tailed unpaired Student's t-test.

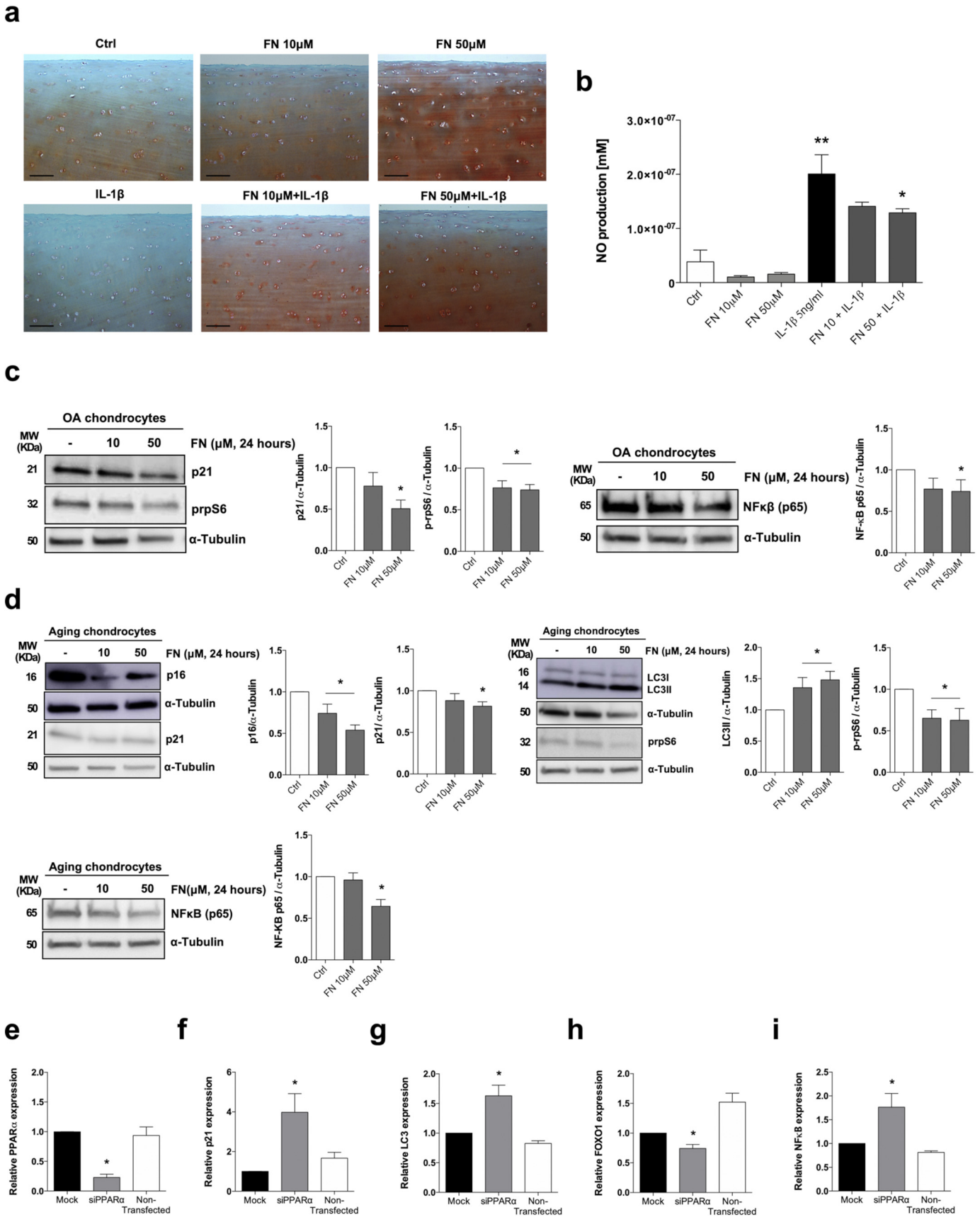
a
Ctrl
FN 10μM
FN 50μM
IL-1β
FN 10μM+IL-1β
FN 50μM+IL-1β
b
NO production [mM]
3.0×10-07
2.0×10-07
1.0×10-07
0
**
*
Ctrl
FN 10μM
FN 50μM
IL-1β 5ng/ml
FN 10 + IL-1β
FN 50 + IL-1β
c
OA chondrocytes
MW (KDa)
- 10 50
FN (μM, 24 hours)
21
p21
32
prpS6
50
α-Tubulin
p21/ α-Tubulin
p-rpS6 / α-Tubulin
OA chondrocytes
MW (KDa)
- 10 50
FN (μM, 24 hours)
65
NFκβ (p65)
50
α-Tubulin
NF-κB p65 / α-Tubulin
Ctrl
FN 10μM
FN 50μM
d
Aging chondrocytes
MW (KDa)
- 10 50
FN (μM, 24 hours)
16
p16
α-Tubulin
21
p21
50
α-Tubulin
p16/α-Tubulin
p21/ α-Tubulin
Aging chondrocytes
MW (KDa)
- 10 50
FN (μM, 24 hours)
16
14
LC3I
LC3II
50
α-Tubulin
32
prpS6
50
α-Tubulin
LC3II / α-Tubulin
p-rpS6 / α-Tubulin
Aging chondrocytes
MW (KDa)
- 10 50
FN(μM, 24 hours)
65
NFκB (p65)
50
α-Tubulin
NF-KB p65 / α-Tubulin
Ctrl
FN 10μM
FN 50μM
e
Relative PPARα expression
Mock
siPPARα
Non-Transfected
f
Relative p21 expression
Mock
siPPARα
Non-Transfected
g
Relative LC3 expression
Mock
siPPARα
Non-Transfected
h
Relative FOXO1 expression
Mock
siPPARα
Non-Transfected
i
Relative NFκB expression
Mock
siPPARα
Non-Transfected

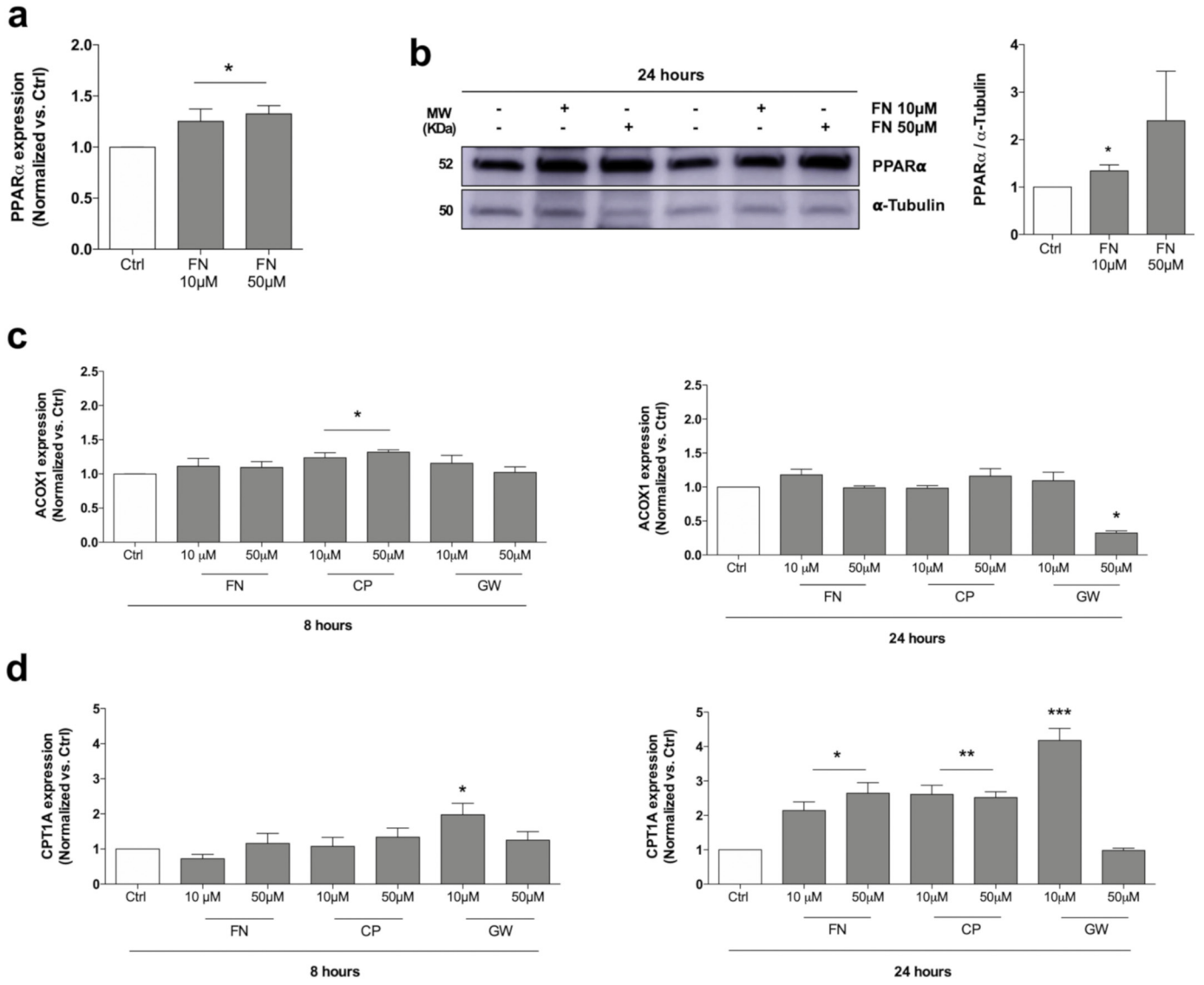

Fig. 8. FN increases PPARα expression and regulates β-oxidation in human chondrocytes. a. Relative expression of PPARα in T/C28a2 human chondrocytes untreated or treated with FN (10, 50 μM) for 24 h. Values are mean ± SEM of 3 independent observations, *$p < .05$ *vs. Ctrl*, two-tailed unpaired Student's t-test. b. Western blot and densitometric analysis of PPARα expression in human OA primary chondrocytes treated with FN (10, 50 μM) for 24 h. Values are mean ± SEM of 3 human donors, *$p < .05$ *vs. Ctrl*, two-tailed unpaired Student's t-test. α-tubulin was employed as a loading control. c. Relative expression of ACOX1 in T/C28a2 human chondrocytes untreated or treated with PPARα agonists FN, CP and GW (10, 50 μM) for 8 and 24 h. Values are mean ± SEM of 3 independent observations (8 h: *$p < .05$ *vs. Ctrl*, two-tailed unpaired Student's t-test; 24 h: *$p < .001$ *vs. Ctrl*, two-tailed unpaired Student's t-test). d. Relative expression of CPT1A in T/C28a2 human chondrocytes untreated or treated with PPARα agonists FN, CP and GW (10, 50 μM) for 8 and 24 h. Values are mean ± SEM of 3 independent observations (8 h: *$p < .05$ *vs. Ctrl*, two-tailed unpaired Student's t-test; 24 h: *$p < .01$, **$p < 0{,}01$, ***$p < .001$ *vs. Ctrl*, two-tailed unpaired Student's t-test).

were taking fenofibrate (FN), ten users (28.6%) were taking gemfibrozil, and one user was initially taking gemfibrozil and then switched to FN. Furthermore, during the follow-up there were 3 (4.3% of the knees) total knee replacements in the fibrate user group and 7 (11.4% of the knees) in the matched control group, respectively. Interestingly, the results indicate that fibrate use by time interaction was associated with a statistically significant improvement of WOMAC function and WOMAC total scores. There was also a trend towards a decrease in WOMAC pain score. The results suggest that the fibrate use, when compared with non-use, was associated with an average yearly decrease in WOMAC function grade by 1.15 and WOMAC total score by 1.6, as reflected by β-coefficients of 1.15 and 1.6, respectively (Fig. 10d).

Fig. 7. FN regulates senescence, autophagy and cartilage degradation in human chondrocytes and cartilage. a. Safranin O–stained sections representative of $n = 3$ human ageing cartilage donors treated with FN (10, 50 μM), IL-1β (5 ng/ml) or in combination for 72 h. Scale bar, 10 μm. b. Nitric oxide (NO) production into supernatants from human ageing chondrocytes treated with FN (10, 50 μM), IL-1β (5 ng/ml) or in combination for 24 h. Values are mean ± SEM of $n = 5$ human donors. *$p < .05$ *vs. IL-1β*, **$p < .05$ *vs. Ctrl*, two-tailed unpaired Student's t-test. c. Western blot and densitometric analysis of p21, prbS6 and NFκB expression in human OA primary chondrocytes treated with FN (10, 50 μM) for 24 h. α-tubulin was employed as a loading control. Values are mean ± SEM of $n = 3$ human donors for p21 and $n = 4$ human donors for prbS6 and NFκβ, *$p < .05$ *vs. Ctrl*, two-tailed unpaired Student's t-test. d. Western blot and densitometric analysis of p16, p21, LC3II, prbS6 and NFκB expression in human ageing primary chondrocytes treated with FN (10, 50 μM) for 24 h. α-tubulin was employed as a loading control. Values are mean ± SEM of $n = 6$ human donors for p16 and p21; $n = 5$ for LC3 and prbS6, *$p < .05$ *vs. Ctrl*; $n = 4$ for NFκB, *$p < .01$ *vs. Ctrl*, two-tailed unpaired Student's t-test. e-i, Relative expression of *PPARα*, *p21*, *LC3*, *FOXO1* and *NFκB*, in T/C28a2 human chondrocytes subjected to genetic deletion of PPARα. Values are mean ± SEM. *PPARα:* *$p < .05$, n = 3 independent observations, p21: *$p < .05$, n = 4 independent observations, LC3: *$p < .05$, n = 3 independent observations, FOXO1: *$p < .01$, $n = 6$, *NFκB:* *$p < .05$, n = 4 independent observations *vs. Mock*, two-tailed unpaired Student's t-test.

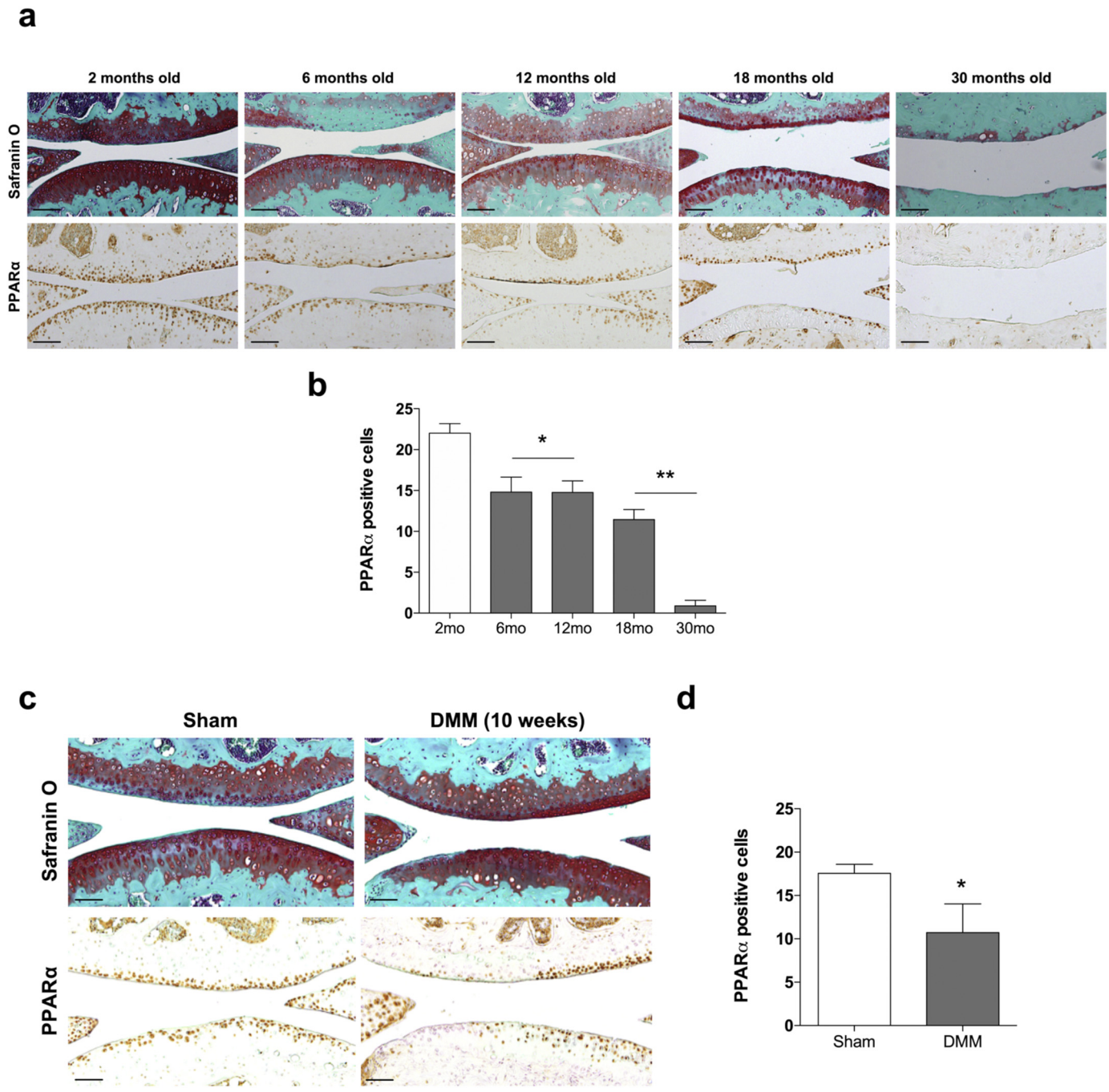

Fig. 9. PPARα is downregulated with ageing and OA in mice. a. Knee joint sections from C57Bl6/J were analysed by immunohistochemistry for PPARα. Representative images of knee joints from 2, 6, 12, 18 and 30-month-old mice stained with Safranin O-Fast Green and PPARα. Scale bar, 10 μm. b, Quantitative analysis of PPARα-positive cells. Values are the mean ± SEM of 3 mice per group. $^{*}p < .05$; $^{**}p < .0001$ *vs. 2-month-old mice*, two-tailed unpaired Student's t-test. c, Reduction in PPARα expression in knee joints from mice with surgically induced osteoarthritis (OA). Knee joints from 6-month-old C57BL/6 J mice that underwent sham surgery and from mice 10 weeks after surgical OA induced by transection of the medial meniscotibial ligament and the medial collateral ligament (DMM), analysed using Safranin O staining for expression of PPARα. Scale bar, 10 μm. d, Quantification of PPARα-positive cells. Values are the mean ± SEM of 4 mice per group. $^{*}p < .05$ *vs. Sham*, two-tailed unpaired Student's t-test.

4. Discussion

Disease-modifying therapeutic agents to prevent or stop progression of OA are an urgent clinical need. Recent data support that selective targeting of senescent chondrocytes with small molecules is an effective therapy in preclinical models of OA [14]. Activation of autophagy prevents against chondrocyte death, cartilage ageing and OA [21,22]. We hypothesized that simultaneously targeting senescence and autophagy in chondrocytes might be a useful strategy to identify therapeutic agents for joint ageing and OA. Here, we have identified PPARα activation as a dual senolytic / autophagy enhancing strategy by using a human chondrocyte cell-based phenotypic screening assay. Senescence was induced by treatment with SASP factor IL-6 [53], increasing SA-β-Gal activity and p21 expression, while decreasing autophagic flux and inducing the mTOR signalling pathway. Paracrine exposure of chondrocytes to IL-6 likely resembles some of the early ageing and cartilage degeneration signalling events which were considered key in OA development. These results also suggest an interesting homeostatic imbalance, whereby IL-6-induced inflammation and senescence is accompanied by decreased autophagy in chondrocytes. This observation

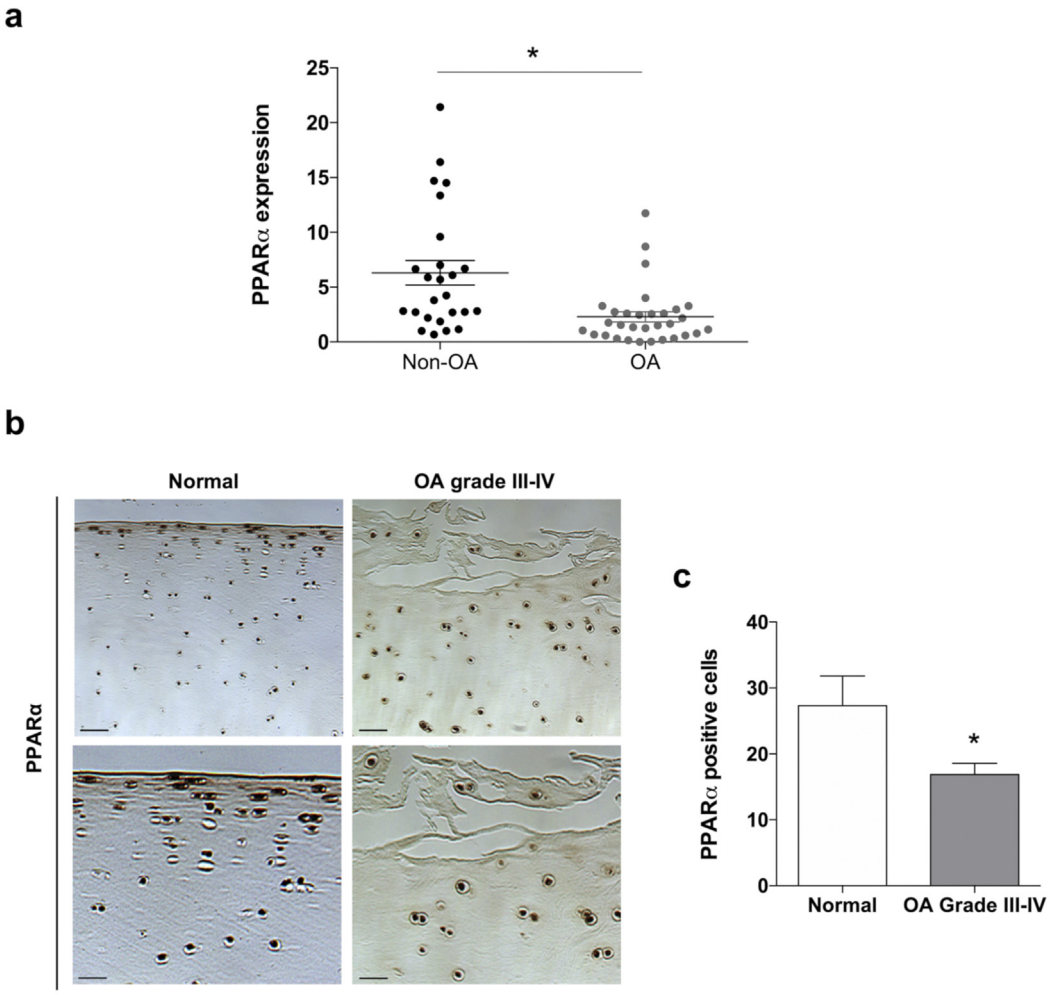

d

Table 2. Longitudinal analysis (with treatment* interaction) of WOMAC subcategories and fibrates use

WOMAC index	β-coeficient	95% CI	Pvalue
WOMAC Pain	-0.3	-0.63 to -0.035	0.08
WOMAC Function	-1.15	-2.1 to -0.2	0.018
WOMAC Stiffness	-0.07	-0.23 to 0.1	0.43
WOMAC Total	-1.6	-2.93 to -0.21	0.024

WOMAC, Western Ontario and McMaster Universities OA index; **CI**, 95% confidence interval

Fig. 10. PPARα is downregulated in blood and cartilage from OA patients. a. Relative expression of PPARα in blood from non-OA and OA patients from OA cohort, PROCOAC. Values are mean ± SEM of $n = 25$ non-OA patients and $n = 30$ Knee OA patients, $^{*}p < .001$ *vs. non-OA*, two-tailed unpaired Student's t-test. b. Human Normal and OA cartilage was analysed by immunohistochemistry for PPARα. Representative images of normal and OA cartilage stained with PPARα. Scale bar, 10 μm. c, Quantitative analysis of PPARα-positive cells. Values are the mean ± SEM of n = 5 human donors per group. $^{*}p < .05$ *vs. normal*, two-tailed unpaired Student's t-test. d, Longitudinal analysis (with treatment* time interaction) of WOMAC subcategories and fibrates use.

reflects a complex interplay between elevated senescence and decreased autophagy that can promote cartilage disease.

Our cell-based screening assay yielded a number of drugs with different mechanism of actions potentially interacting with OA pathogenesis pathways. A number of ion channels and pumps disruptors were identified. Since hormones, growth factors, cytokines, and eicosanoids are critical signals for mainteinance of chondrocyte homeostasis, the PPARα nuclear receptor was of prime interest because is an established modulator of lipid metabolism and its role in the inflammatory mechanism can explain the positive impact in cartilage homeostasis [54,55]. Indeed, it has been demonstrated that PPARγ has a protective role in articular cartilage. Cartilage-specific PPARγ deficient mice showed increased apoptosis as well as production of inflammatory and catabolic factors, and a decreased expression of anabolic factors, overall resulting in accelerated OA [56,57]. Here, we have demonstrated that the PPARα agonist fenofibrate (FN) significantly reduced chondrocyte senescence and induced autophagic flux significantly, indicating a partial reversion of the chondrocyte age-related phenotype.

Our results demonstrate that PPARα ligands selectively eliminate senescent chondrocytes *via* cell death through apoptosis [4]. In addition,

PPARα agonists induced autophagic flux, mediated by a related increase in cell homeostasis markers, such as LC3 and FoxO1. Moreover, treating OA and ageing chondrocytes with fenofibrate results in abrogation of the active, phosphorylated form of the mTOR effector S6 Ribosomal Protein. Senescent cells are prone to anti-apoptotic signals and show irreversible proliferative arrest [58]. Downregulation of this proliferation pathway may contribute to the senolytic activity of PPARα ligands, however, further work using PPARα ligands is required to establish how nuclear receptor signalling remodels cartilage metabolism and the full range of signalling it regulates.

To investigate the relevance of PPARα as a therapeutic target, we explore whether its genetic deletion could affect critical chondrocyte survival mechanisms. We found that PPARα deficient human chondrocytes were susceptible to senescence, increased expression of inflammation mediators and to changes in homeostasis by a reduction of FoxO1 expression and an increase in LC3, which might act as a regulator of lipid signals influencing homeostasis. These results highlight the importance of PPARα in maintenance of chondrocyte homeostasis.

Since PPARα regulates peroxisomal and mitochondrial fatty acid β-oxidation [59], the effect of PPARα agonists in human chondrocytes also was evaluated. The results showed an increase in expression of CPT1A expression, a target gene of PPARα [60], suggesting that these ligands regulate mitochondrial fatty acid β-oxidation in human chondrocytes. These results are consistent with a positive remodelling of cartilage metabolism that protects against ageing and disease signals.

PPARα was found to be downregulated in spontaneous ageing-related and surgically induced OA mouse models, as well as in blood and cartilage from patients with knee OA, indicating an intrinsic OA-related PPARα defect. Importantly, pharmacological activation of PPARα by fibrate treatment in human OA patients was associated with a significant decrease in progressive disability and a trend towards a decrease in knee pain. There were fewer joint replacement surgeries in patients taking fibrates. These findings are in line with an open label study performed on patients with erosive hand OA where FN use for 12 weeks was associated with significant improvements in the Cochin hand functional disability scale [61]. In another exploratory study carried out through the OAI database, neither reduced radiographic progression nor reduction in worsening of pain in participants taking fibrates were detected. The authors did not assess the effects of fibrates on disability and used a prevalent user design (*i.e.* included participants who used fibrates at baseline) [62] that may be associated with bias [63] and may account for the non-detection of fibrate effect on pain. It is difficult to interpret the dissociation of fibrate effects on disability and pain found in this analysis as pain and functional limitation in knee OA are closely related [64]. As anxiety has been shown to be one of the determinants of functioning in knee OA [65], one of the explanations of the reduction in disability found in the present study may be the observed emerging anxiolytic effects of PPARα agonism [66]. On the other hand, the lack of association between fibrate use and pain reduction may be due to absence of analgesic properties of PPARα agonists or may be due to reduced statistical power caused by small sample size.

These clinical findings support the hypothesis that fibrates may improve joint function in human OA patients and encourage further prospective and conclusive studies to demonstrate the value of fibrates as disease modifying OA therapy.

In conclusion, regulation of lipid metabolism by PPARα can be considered as a potential therapeutic target for OA.

Acknowledgements

We thank the staff of the Orthopedic Department of the Complejo Hospitalario Universitario A Coruña for providing the cartilage samples. Furthermore, we thank Tamara Hermida and Merissa Olmer for technical assistance and Richard Roberts for editing the revised manuscript in British English.

The OAI is a public-private partnership comprising five contracts (N01-AR-2-2258; N01-AR-2-2259; N01-AR-2-2260; N01-AR-2-2261; N01-AR-2-2262) funded by the National Institutes of Health, a branch of the Department of Health and Human Services, and conducted by the OAI Study Investigators. Private funding partners include Merck Research Laboratories, Novartis Pharmaceuticals Corporation, GlaxoSmithKline and Pfizer, Inc. Private sector funding for the OAI is managed by the Foundation for the National Institutes of Health. This manuscript was prepared using an OAI public use data set and does not necessarily reflect the opinions or views of the OAI investigators, the NIH or the private funding partners.

Funding sources

This study was supported by Instituto de Salud Carlos III- Ministerio de Ciencia, Innovación y Universidades, Spain, Plan Estatal 2013-2016 and Fondo Europeo de Desarrollo Regional (FEDER), *"Una manera de hacer Europa"*, PI14/01324 and PI17/02059, by Innopharma Pharmacogenomics platform applied to the validation of targets and discovery of drugs candidates to preclinical phases, Ministerio de Economía y Competitividad, by grants of the National Institutes of Health to PDR (P01 AG043376 and U19 AG056278). We thank the FOREUM Foundation for Research in Rheumatology for their support. UNR was supported by Programa Operativo FSE Galicia 2014–2020, Xunta de Galicia, Spain, BC was supported by Miguel Servet Type II Program-CPII16/00045-A, Instituto de Salud Carlos III, Ministerio de Ciencia, Innovación y Universidades, Spain. The funders had no role in study design, data collection and analysis, decision to publish, or preparation of the manuscript.

Conflicts of interest

The authors have declared no potential conflicts of interest.

Author's contributions

All authors approved the final version to be published.

Concept and design: Domínguez, Caramés.

Performed the experiments: Nogueira-Recalde, Lorenzo-Gómez, Grassi, Domínguez, Caramés.

Data analysis and interpretation: Nogueira-Recalde, Domínguez, Caramés.

Writing and review of Manuscript: Nogueira-Recalde, Blanco, Loza, Shirinsky, Lotz, Robbins, Domínguez and Caramés.

Appendix A. Supplementary data

Supplementary data to this article can be found online at https://doi.org/10.1016/j.ebiom.2019.06.049.

References

[1] Lopez-Otin C, Blasco MA, Partridge L, Serrano M, Kroemer G. The hallmarks of aging. Cell 2013;153(6):1194–217.
[2] Lotz MK, Carames B. Autophagy and cartilage homeostasis mechanisms in joint health, aging and OA. Nat Rev Rheumatol 2011;7(10):579–87.
[3] Wang R, Yu Z, Sunchu B, et al. Rapamycin inhibits the secretory phenotype of senescent cells by a Nrf2-independent mechanism. Aging Cell 2017;16(3):564–74.
[4] van Deursen JM. The role of senescent cells in ageing. Nature 2014;509(7501):439–46.
[5] Baker DJ, Childs BG, Durik M, et al. Naturally occurring p16(Ink4a)-positive cells shorten healthy lifespan. Nature 2016;530(7589):184–9.
[6] Xu M, Pirtskhalava T, Farr JN, et al. Senolytics improve physical function and increase lifespan in old age. Nat Med 2018;24(8):1246–56.
[7] Campisi J. Aging and cancer: the double-edged sword of replicative senescence. J Am Geriatr Soc 1997;45(4):482–8.
[8] Abramson SB, Attur M, Amin AR, Clancy R. Nitric oxide and inflammatory mediators in the perpetuation of osteoarthritis. Curr Rheumatol Rep 2001;3(6):535–41.

[9] Zhou HW, Lou SQ, Zhang K. Recovery of function in osteoarthritic chondrocytes induced by p16INK4a-specific siRNA in vitro. Rheumatology (Oxford) 2004;43(5):555–68.
[10] Price JS, Waters JG, Darrah C, et al. The role of chondrocyte senescence in osteoarthritis. Aging Cell 2002;1(1):57–65.
[11] Benderdour M, Martel-Pelletier J, Pelletier JP, Kapoor M, Zunzunegui MV, Fahmi H. Cellular aging, senescence and autophagy processes in osteoarthritis. Curr Aging Sci 2015;8(2):147–57.
[12] Diekman BO, Sessions GA, Collins JA, et al. Expression of p16(INK)(4a) is a biomarker of chondrocyte aging but does not cause osteoarthritis. Aging Cell Aug 2018;17(4):e12771.
[13] Xu M, Bradley EW, Weivoda MM, et al. Transplanted senescent cells induce an osteoarthritis-like condition in mice. J Gerontol Series A 2017;72(6):780–5.
[14] Jeon OH, Kim C, Laberge RM, et al. Local clearance of senescent cells attenuates the development of post-traumatic osteoarthritis and creates a pro-regenerative environment. Nat Med 2017;23(6):775–81.
[15] Musumeci G, Castrogiovanni P, Trovato FM, et al. Physical activity ameliorates cartilage degeneration in a rat model of aging: a study on lubricin expression. Scand J Med Sci Sports 2015;25(2):e222–30.
[16] Justice JN, Nambiar AM, Tchkonia T, et al. Senolytics in idiopathic pulmonary fibrosis: results from a first-in-human, open-label, pilot study. EBioMedicine 2019;40:554–63.
[17] Ogrodnik M, Salmonowicz H, Gladyshev VN. Integrating cellular senescence with the concept of damage accumulation in aging: relevance for clearance of senescent cells. Aging Cell 2019;18(1):e12841.
[18] Mobasheri A, Matta C, Zakany R, Musumeci G. Chondrosenescence: definition, hallmarks and potential role in the pathogenesis of osteoarthritis. Maturitas 2015;80(3):237–44.
[19] Musumeci G, Szychlinska MA, Mobasheri A. Age-related degeneration of articular cartilage in the pathogenesis of osteoarthritis: molecular markers of senescent chondrocytes. Histol Histopathol 2015;30(1):1–12.
[20] Vinatier C, Dominguez E, Guicheux J, Carames B. Role of the inflammation-autophagy-senescence integrative network in osteoarthritis. Front Physiol 2018;9:706.
[21] Carames B, Taniguchi N, Otsuki S, Blanco FJ, Lotz M. Autophagy is a protective mechanism in normal cartilage, and its aging-related loss is linked with cell death and osteoarthritis. Arthritis Rheum 2010;62(3):791–801.
[22] Carames B, Olmer M, Kiosses WB, Lotz MK. The relationship of autophagy defects to cartilage damage during joint aging in a mouse model. Arthrit Rheumatol (Hoboken, NJ) 2015;67(6):1568–76.
[23] Kroemer G. Autophagy: a druggable process that is deregulated in aging and human disease. J Clin Invest 2015;125(1):1–4.
[24] Leidal AM, Levine B, Debnath J. Autophagy and the cell biology of age-related disease. Nat Cell Biol 2018;20(12):1338–48.
[25] Maiuri MC, Kroemer G. Therapeutic modulation of autophagy: which disease comes first? Cell Death Differ 2019;26(4):680–9.
[26] Matsuzaki T, Alvarez-Garcia O, Mokuda S, et al. FoxO transcription factors modulate autophagy and proteoglycan 4 in cartilage homeostasis and osteoarthritis. Sci Transl Med 2018;10(428).
[27] Zhang Z, Yao Z, Zhao S, et al. Interaction between autophagy and senescence is required for dihydroartemisinin to alleviate liver fibrosis. Cell Death Dis 2017;8(6):e2886.
[28] Fuhrmann-Stroissnigg H, Ling YY, Zhao J, et al. Identification of HSP90 inhibitors as a novel class of senolytics. Nat Commun 2017;8(1):422.
[29] Coleman DT, Gray AL, Stephens CA, Scott ML, Cardelli JA. Repurposed drug screen identifies cardiac glycosides as inhibitors of TGF-beta-induced cancer-associated fibroblast differentiation. Oncotarget 2016;7(22):32200–9.
[30] Druzhyna N, Szczesny B, Olah G, et al. Screening of a composite library of clinically used drugs and well-characterized pharmacological compounds for cystathionine beta-synthase inhibition identifies benserazide as a drug potentially suitable for repurposing for the experimental therapy of colon cancer. Pharmacol Res 2016;113:18–37 Pt A.
[31] Varbanov HP, Kuttler F, Banfi D, Turcatti G, Dyson PJ. Repositioning approved drugs for the treatment of problematic cancers using a screening approach. PLoS One 2017;12(2):e0171052.
[32] Hulsmans M, Geeraert B, Arnould T, Tsatsanis C, Holvoet P. PPAR agonist-induced reduction of Mcp1 in atherosclerotic plaques of obese, insulin-resistant mice depends on adiponectin-induced Irak3 expression. PLoS One 2013;8(4):e62253.
[33] Goldring MB, Birkhead JR, Suen LF, et al. Interleukin-1 beta-modulated gene expression in immortalized human chondrocytes. J Clin Invest 1994;94(6):2307–16.
[34] Fernandez-Moreno M, Soto-Hermida A, Vazquez-Mosquera ME, et al. A replication study and meta-analysis of mitochondrial DNA variants in the radiographic progression of knee osteoarthritis. Rheumatology (Oxford) 2017;56(2):263–70.
[35] Zhang JH, Chung TD, Oldenburg KR. A simple statistical parameter for use in evaluation and validation of high throughput screening assays. J Biomol Screen 1999;4(2):67–73.
[36] Gump JM, Thorburn A. Sorting cells for basal and induced autophagic flux by quantitative ratiometric flow cytometry. Autophagy 2014;10(7):1327–34.
[37] Ribeiro M, Lopez de Figueroa P, Blanco FJ, Mendes AF, Carames B. Insulin decreases autophagy and leads to cartilage degradation. Osteoarthr Cartil 2016;24(4):731–9.
[38] Glasson SS, Chambers MG, Van Den Berg WB, Little CB. The OARSI histopathology initiative - recommendations for histological assessments of osteoarthritis in the mouse. Osteoarthr Cartil 2010;18(Suppl. 3):S17–23.
[39] Taniguchi N, Carames B, Ronfani L, et al. Aging-related loss of the chromatin protein HMGB2 in articular cartilage is linked to reduced cellularity and osteoarthritis. Proc Natl Acad Sci U S A 2009;106(4):1181–6.
[40] Washburn RA, Smith KW, Jette AM, Janney CA. The physical activity scale for the elderly (PASE): development and evaluation. J Clin Epidemiol 1993;46(2):153–62.
[41] Bellamy N, Buchanan WW, Goldsmith CH, Campbell J, Stitt LW. Validation study of WOMAC: a health status instrument for measuring clinically important patient relevant outcomes to antirheumatic drug therapy in patients with osteoarthritis of the hip or knee. J Rheumatol 1988;15(12):1833–40.
[42] Pahor M, Chrischilles EA, Guralnik JM, Brown SL, Wallace RB, Carbonin P. Drug data coding and analysis in epidemiologic studies. Eur J Epidemiol 1994;10(4):405–11.
[43] Diamond A, Sekhon JS. Genetic matching for estimating causal effects: a general multivariate matching method for achieving balance in observational studies. Rev Econ Stat 2013;95(3):932–45.
[44] Stuart EA. Matching methods for causal inference: a review and a look forward. Stat Sci 2010;25(1):1–21.
[45] Austin PC. Balance diagnostics for comparing the distribution of baseline covariates between treatment groups in propensity-score matched samples. Stat Med 2009;28(25):3083–107.
[46] Twisk J, de Vente W. Attrition in longitudinal studies. How to deal with missing data. J Clin Epidemiol 2002;55(4):329–37.
[47] Ho DE, Imai K, King G, Stuart EA. MatchIt: nonparametric preprocessing for parametric causal inference. J Stat Softw 2011;42(8).
[48] Carey Vincent J. Gee: Generalized estimation equation solver. https://CRAN.R-project.org/package=gee; 2015.
[49] Milanovic M, Fan DNY, Belenki D, et al. Senescence-associated reprogramming promotes cancer stemness. Nature 2018;553(7686):96–100.
[50] Xie X, Hu H, Tong X, et al. The mTOR-S6K pathway links growth signalling to DNA damage response by targeting RNF168. Nat Cell Biol 2018;20(3):320–31.
[51] Yousefzadeh MJ, Zhu Y, McGowan SJ, et al. Fisetin is a senotherapeutic that extends health and lifespan. EBioMedicine Oct 2018;36:18–28.
[52] Tyagi S, Gupta P, Saini AS, Kaushal C, Sharma S. The peroxisome proliferator-activated receptor: a family of nuclear receptors role in various diseases. J Adv Pharm Technol Res 2011;2(4):236–40.
[53] Kojima H, Inoue T, Kunimoto H, Nakajima K. IL-6-STAT3 signaling and premature senescence. Jak-stat 2013;2(4):e25763.
[54] Narala VR, Adapala RK, Suresh MV, Brock TG, Peters-Golden M, Reddy RC. Leukotriene B4 is a physiologically relevant endogenous peroxisome proliferator-activated receptor-alpha agonist. J Biol Chem 2010;285(29):22067–74.
[55] Clockaerts S, Bastiaansen-Jenniskens YM, Feijt C, et al. Peroxisome proliferator activated receptor alpha activation decreases inflammatory and destructive responses in osteoarthritic cartilage. Osteoarthr Cartil 2011;19(7):895–902.
[56] Vasheghani F, Monemdjou R, Fahmi H, et al. Adult cartilage-specific peroxisome proliferator-activated receptor gamma knockout mice exhibit the spontaneous osteoarthritis phenotype. Am J Pathol 2013;182(4):1099–106.
[57] Vasheghani F, Zhang Y, Li YH, et al. PPARgamma deficiency results in severe, accelerated osteoarthritis associated with aberrant mTOR signalling in the articular cartilage. Ann Rheum Dis 2015;74(3):569–78.
[58] Kirkland JL, Tchkonia T. Cellular senescence: a translational perspective. EBioMedicine 2017;21:21–8.
[59] Mascaro C, Acosta E, Ortiz JA, Marrero PF, Hegardt FG, Haro D. Control of human muscle-type carnitine palmitoyltransferase I gene transcription by peroxisome proliferator-activated receptor. J Biol Chem 1998;273(15):8560–3.
[60] Xiao Y, Wang J, Yan W, Zhou K, Cao Y, Cai W. p38alpha MAPK antagonizing JNK to control the hepatic fat accumulation in pediatric patients onset intestinal failure. Cell Death Dis 2017;8(10):e3110.
[61] Shirinsky IV, Shirinsky VS. Treatment of erosive osteoarthritis with peroxisome proliferator-activated receptor alpha agonist fenofibrate: a pilot study. Rheumatol Int 2014;34(5):613–6.
[62] Driban JB, Lo GH, Eaton CB, et al. Exploratory analysis of osteoarthritis progression among medication users: data from the osteoarthritis initiative. Ther Adv Musculoskelet Dis 2016;8(6):207–19.
[63] Ray WA. Evaluating medication effects outside of clinical trials: new-user designs. Am J Epidemiol 2003;158(9):915–20.
[64] McAlindon TE, Cooper C, Kirwan JR, Dieppe PA. Determinants of disability in osteoarthritis of the knee. Ann Rheum Dis 1993;52(4):258–62.
[65] Creamer P, Lethbridge-Cejku M, Hochberg MC. Factors associated with functional impairment in symptomatic knee osteoarthritis. Rheumatology (Oxford) 2000;39(5):490–6.
[66] Nisbett KE, Pinna G. Emerging therapeutic role of PPAR-alpha in cognition and emotions. Front Pharmacol 2018;9:998.